Volume 61
Number 72
16 September 2025
Pages 13491–13732

ChemComm

Chemical Communications

rsc.li/chemcomm

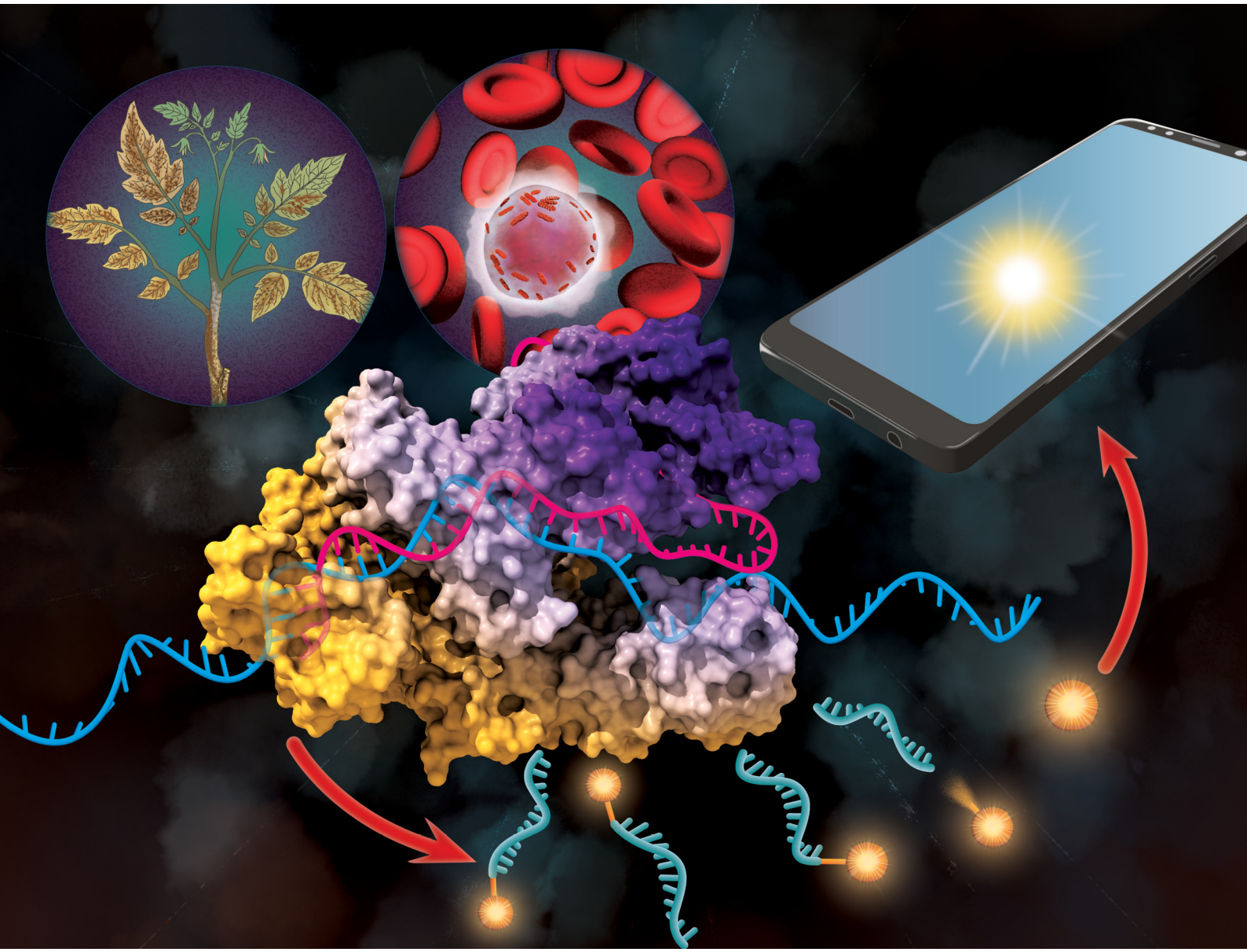

ISSN 1359-7345

ROYAL SOCIETY OF CHEMISTRY

FEATURE ARTICLE

Qingshan Wei *et al.*

CRISPR–Cas based platforms for RNA detection: fundamentals and applications

ChemComm

ROYAL SOCIETY OF CHEMISTRY

FEATURE ARTICLE

View Article Online
View Journal | View Issue

Cite this: *Chem. Commun.*, 2025, **61**, 13571

CRISPR–Cas based platforms for RNA detection: fundamentals and applications

Mahsa Bagi, Sina Jamalzadegan, Anastasiia Steksova and Qingshan Wei *

The detection of RNA biomarkers is crucial for diagnosing many urgent diseases such as infections and cancer. Conventional RNA detection techniques such as RT-PCR, LAMP, and microarrays are effective, but often face limitations in terms of speed, sensitivity, and equipment demands. In recent years, CRISPR/Cas systems have emerged as versatile platforms for RNA detection, which offer high specificity, programmability, and adaptability across a wide range of diagnostic applications. This review first categorizes different CRISPR-based RNA detection systems according to the CRISPR effectors employed, including Cas13, Cas12, Cas14, Cas9, and newly characterized enzymes such as Cas7–11 and Cas10, detailing their mechanisms of target recognition, cleavage activity, and signal generation. The CRISPR detection platforms are coupled with or without pre-amplification steps to meet the different sensitivity needs. Preamplification-based systems integrate CRISPR with methods like RT-PCR and isothermal amplification to enhance sensitivity. In parallel, preamplification-free strategies, such as split-crRNA or split-activator systems, are gaining attention for their balanced assay performance and simplicity, which are especially attractive for point-of-care (POC) settings. Then, the diagnostic applications of these technologies are explored across two major domains: infectious disease detection and cancer biomarker identification *via* miRNAs, demonstrating the clinical potential of CRISPR-based RNA detection platforms. In addition, we explore ongoing challenges such as improving sensitivity in amplification-free formats, and developing field-deployable, cost-effective systems. The review concludes by outlining emerging trends and future directions in CRISPR-based RNA diagnostics, emphasizing their transformative potential in clinical settings.

Received 9th June 2025,
Accepted 21st July 2025

DOI: 10.1039/d5cc03257a

rsc.li/chemcomm

Introduction

Ribonucleic acid (RNA), known as the intermediate molecule between DNA and protein, serves as a key nucleic acid for tracking cell performance.[1] RNA detection is a versatile tool for monitoring cell status,[2] detection of infectious diseases,[3] as well as for diagnosis of cancer[4] and neurodegenerative[5] diseases by tracking gene expression. It can also be used to evaluate the efficiency of drugs designed to target specific molecular pathways by monitoring RNA molecules, and to confirm the success rate of CRISPR–Cas systems in achieving functional gene editing.

To date, a wide range of RNA detection techniques have been developed to target various RNA types, including microRNAs (miRNAs) and viral RNAs, across both *in vitro* and *in vivo* environments. Among the most commonly used methods are reverse transcription polymerase chain reaction (RT-PCR),[6] quantitative reverse transcription PCR (RT-qPCR),[7] northern blotting,[8] RNA sequencing (RNA-Seq),[9] *in situ* hybridization (ISH),[10] and microarray[11] technologies. Each of these approaches offers distinct advantages, yet they also present notable limitations. Specifically, many of these methods require expensive instrumentation, non-portable setups, labor-intensive protocols, and the expertise of trained laboratory personnel.[12] To overcome these challenges, there is a growing need to develop RNA detection strategies that are compatible with portable, cost-effective, fast-response, and user-friendly devices. These innovations are particularly valuable for critical biomedical and biological applications, including the early diagnosis of viral infections, transcriptomic profiling in cancer and neurodegenerative diseases, and the monitoring of gene expression dynamics in cellular therapies and drug delivery systems. Consequently, advancing rapid and cost-effective RNA detection technologies remains a crucial objective to enhance the accessibility, timeliness, and impact of RNA-based diagnostics and therapeutic monitoring.

Clustered regularly interspaced short palindromic repeats (CRISPR) and CRISPR-associated (Cas) enzymes, first identified in bacteria in 1987,[13] represent a natural defense mechanism against invading genetic elements such as plasmids and phages.[14] The transformative potential of the CRISPR–Cas

Department of Chemical and Biomolecular Engineering, North Carolina State University, Raleigh, NC 27605, USA. E-mail: qwei3@ncsu.edu

system for genome editing was first demonstrated in 2012, when researchers successfully repurposed it for precise and programmable DNA cleavage.[14] Later, around 2016–2017, specific Cas enzymes, particularly Cas13,[15] were shown to possess high efficacy for nucleic acid detection, enabling the direct targeting of RNA molecules and the development of novel RNA-based diagnostic technologies. Compared to conventional RNA detection methods, CRISPR/Cas-based platforms offer rapid, highly sensitive, and highly specific detection that can be integrated into portable biosensor and point-of-care (POC) assay formats.[16–18] Several types of Cas enzymes have been employed for RNA detection depending on whether the strategy relies on direct or indirect detection, pre-amplification-based or amplification-free approaches, and the choice of readout techniques, including fluorescent and non-fluorescent modalities.[19]

Several previous reviews have discussed the applicability of CRISPR-based diagnostic assays for detecting RNA nucleic acids.[20–25] However, many existing works consider RNA detection within the broader context of nucleic acid diagnostics, which, while informative, may not fully elaborate on the unique challenges and strategies pertinent to the diverse array of RNA species, ranging from messenger RNAs (mRNAs), miRNAs, long non-coding RNAs (lncRNAs), to viral RNAs.[21,26] From an experimental perspective, it is also critical to comprehensively discuss both preamplification-free and preamplification-based CRISPR mechanisms for RNA detection. This distinction is crucial for better understanding their respective advantages, limitations, and compatibility with different RNA targets, yet previous reviews often treat these strategies in isolation.[25] In addition, it is important to highlight that CRISPR platforms for RNA detection are relevant not only for pathogenic RNAs, such as viral genomes, but also for non-pathogenic host RNAs that play key roles in complex diseases like cancer and neurodegeneration. Previous reviews, tend to concentrate on pathogen-oriented detection and may overlook other applications.[21,26] Even the more targeted reviews[27] that emphasize Cas13 and modified Cas9 systems for RNA imaging and detection, may not comprehensively address the full range of emerging RNA-targeting Cas effectors or offer a systematic comparison of their molecular mechanisms and application scopes across all RNA classes. As such, there is a need for a timely review that not only introduces CRISPR-based RNA detection as a transformative approach but also systematically categorizes strategies by Cas enzyme and RNA target, delves into their core biological mechanisms and comparative performance, and finally broadly surveys their applications and challenges, thereby bridging fundamental science with real-world utility.

In this review, we first provide an overview of RNA detection and its significance in modern diagnostics, outlining traditional RNA detection methods along with their inherent limitations (Fig. 1). We then introduce CRISPR-based RNA detection as a promising and transformative approach that addresses many of these challenges. Following this, we categorize the various CRISPR-based RNA detection strategies, including platforms built upon various Cas enzymes. For each platform, we comprehensively explore the fundamental biological

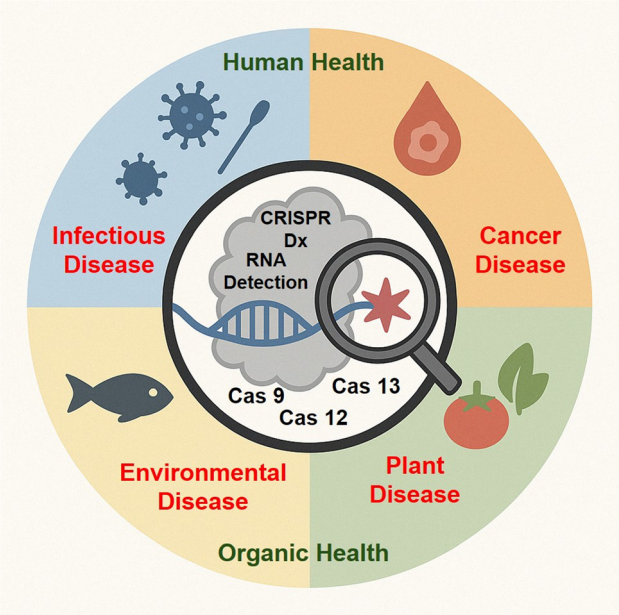

Fig. 1 RNA detection with various CRISPR–Cas systems and their applications in detecting viral RNA and cancer-related RNA biomarkers.

mechanisms involved, distinguishing between preamplification-based and amplification-free detection strategies, and we summarize their unique advantages and disadvantages. Next, we highlight recent applications of CRISPR-based RNA detection across a wide range of fields, from infectious disease diagnostics to cancer biomarker detection, and from neurodegenerative disease monitoring to agricultural and environmental surveillance. Finally, we prospect the current challenges that still limit the widespread adoption of these platforms in real-world applications, considering critical dimensions such as sensitivity, specificity, scalability, and regulatory pathways. We also propose our future perspectives to advance CRISPR/Cas-based RNA detection technologies and bring them closer to their full clinical and environmental potential. To summarize, Sections 1–5 detail various CRISPR–Cas based detection platforms and their characteristics, while Sections 6–8 explore their diverse diagnostic and monitoring applications across different domains.

1. RNA detection using CRISPR–Cas13

The general idea behind CRISPR–Cas diagnostics is based on the activation of the Cas protein upon binding to a specific target. The activation of Cas enzymes will then lead to different types of cleavage behaviors, which are eventually translated into different signal generation for detection. Unlike Cas9 enzymes, which was originally characterized for its site-specific (*cis*) cleavage activity (Fig. 2a) and widely adopted for genome editing applications, Cas12 and Cas13 enzymes are distinguished by their robust *trans*-cleavage activities, a unique feature that has been strategically utilized for nucleic acid detection in molecular diagnostics.[23] The phenomenon of *trans*-cleavage, also known as collateral cleavage, is the core mechanism enabling signal amplification in several leading CRISPR-based diagnostic platforms.

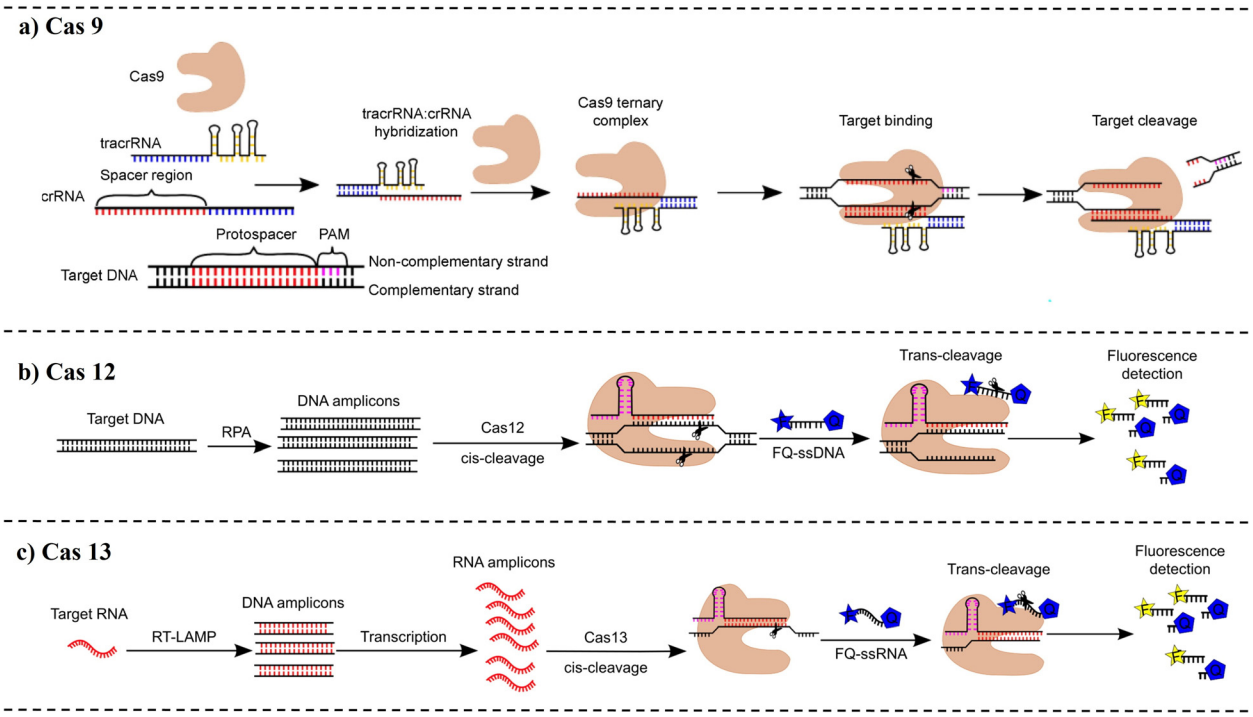

Fig. 2 Detection mechanisms of different Cas effectors. (a) Schematic illustration of Cas 9-based *cis*-cleavage for dsDNA target. (b) Schematic of Cas12-induced *cis*-cleavage and *trans*-cleavage (non-target cleavage) mechanism for dsDNA target detection. (c) Schematic of Cas13-assisted *cis*-cleavage and *trans*-cleavage (non-target cleavage) for ssRNA target detection.[17]

Depending on the Cas enzyme involved, the molecular basis and substrate specificity of this non-specific nuclease activity differ. For Cas12 enzymes, such as Cas12a and Cas12b classes, the guide RNA-directed recognition of a specific DNA target activates the enzyme's single RuvC nuclease domain. This activation not only results in cleavage of the intended double-stranded DNA (dsDNA) target (*cis*-cleavage) but also unleashes an indiscriminate nuclease activity (*trans*-cleavage) that degrades surrounding, non-target single-stranded DNA (ssDNA) molecules[28] (Fig. 2b). Also, Cas14 enzymes, are RNA-guided nucleases that specifically recognize ssDNA targets, and upon binding, activate a collateral cleavage mechanism that indiscriminately degrades nearby non-target ssDNA molecules.[29]

In contrast, the Cas13 family exclusively targets RNA. Upon recognition of its specific single-stranded RNA (ssRNA) target, Cas13's two HEPN (higher eukaryotes and prokaryotes nucleotide-binding) domains become catalytically active, triggering promiscuous degradation of surrounding non-target ssRNA (Fig. 2c). This *trans*-cleavage property is utilized in diagnostic platforms by introducing engineered reporter RNA molecules, the cleavage of which produces a detectable signal, such as fluorescence or a colorimetric change.[28] Cas13-based diagnostics first emerged with the SHERLOCK system developed by Zhang's group in 2017 and have since evolved significantly, with numerous amplification strategies developed to improve sensitivity and adaptability for different applications.[30]

1.1. Preamplification-based RNA detection. While Cas13 itself offers a powerful mechanism for signal generation, many detection platforms incorporate a nucleic acid preamplification step to improve sensitivity, especially when working with low-abundance RNA targets. Preamplification not only increases the quantity of target nucleic acids but also facilitates easier activation of Cas13 enzymes by generating more substrates. One such approach is SATCAS, developed by Ting Wang *et al.* in 2024,[31] which combines simultaneous amplification and testing (SAT) reactions with Cas13a-mediated cleavage in a single-pot system (Table 1). The process begins with reverse transcription of the RNA target into complementary DNA (cDNA), followed by hybridization and extension using specific primers. A T7 promoter is introduced during this stage, enabling the newly synthesized double-stranded DNA to undergo transcription by T7 RNA polymerase, resulting in abundant RNA products. Each template can yield hundreds to thousands of RNA copies, which are then recognized by Cas13a. Cas13a's *trans*-cleavage activity is triggered, and it is able to cut RNA reporter molecule, releasing a fluorescence signal. This integrated and efficient system achieved a limit of detection (LOD) as low as 0.1 aM in 40 minutes, showing its potential for rapid and sensitive viral diagnostics.

Building on the same principle of integrating isothermal amplification with Cas13 detection, Xiao Wang *et al.* in 2024[32] reported a system for detecting synthetic monkeypox virus (MPXV) using recombinase-aided amplification (RAA) followed by T7 transcription and Cas13a–crRNA targeting (Fig. 3d). The output relies on a fluorogenic RNA aptamer (mango III), which emits fluorescence upon binding to the TO3 fluorophore. When Cas13a remains inactive, the aptamer stays intact, and fluorescence is observed. However, if the target is present, Cas13a

Table 1 CRISPR–Cas13-based RNA detection methods integrated with various preamplification strategies

Type of enzyme	Preamplification	Target	LOD	Read out	Rxn time	Ref.
LbuCas13a	RT-PCR	SARS-CoV-2	10 nM	Lateral flow and flour-plate reader	~90 min for fluorescence 35 min for lateral flow	41
Cas13a	RT-PCR	SARS-CoV-2 RNA, HBV RNA, LMP1 gene of EBV, EBNA gene of EBV	0.1 aM	Fluorescence (naked eye under blue light)	40 min	31
LbuCas13a	RT-PCR	SARS-CoV-2	2 aM	Fluorescence, colorimetric, or electrochemical methods	90 min	42
Cas13a	RT-PCR, RT-RAA	Hepatitis delta virus (HDV)	10 copies per μL	Fluorescence and lateral flow strip	60 min for fluorescence; 33 min for lateral flow	43
LwaCas13a	LAMP	miRNA-7 (ciRS-7)	1 fM	Fluorescence	30 min	44
LwCas13a	RT-LAMP	SARS-CoV-2	42 copies per reaction	Fluorescence, lateral flow	70 min	45
Cas13	RT-RPA	Mitochondrial DNA or RNA, reverse transcription of environmental RNA (eRNA)	22.6 ng μL^{-1}	Lateral flow/flour-plate reader	60 min	46
LwCas13a	RPA	*Y. ruckeri* DNA and transcripts sRNAs	2 fM	Fluorescence or lateral flow	70 min	47
LwaCas13a	RPA	*V. alginolyticus*	10 copies per μL	Fluorescence or lateral flow	50 min	48
LwaCas13a	RT-RPA	*Fusarium graminearum* and *Fusarium verticillioides*	Few copies of DNA/RNA targets	Fluorescence, lateral flow	26 min	49
LwaCas13a	CHA	SARS-CoV-2	84 aM	Fluorescence	45 min	50
Cas13a	CHA, HCR	SARS-CoV-2	285 fM	Fluorescence	70 min	51
Cas13a	HCR	Biomarker such as brain natriuretic peptide (BNP)	3.2 fg mL^{-1}	Electrochemiluminescence (ECL)	80 min	52
LbuCas13a	bHCR	miRNA-106a	8.55 aM	Polyacrylamide gel electrophoresis (PAGE), fluorescence and SERS	60 min	36
LwaCas13a	CHDC	miRNA-17, miRNA-155, TTF-1 mRNA, miRNA-19b, miRNA-210 and EGFR mRNA	50 aM	Electrochemical biosensor	36 min	33
Cas13a	Endonuclease-mediated cyclic fluorescent amplification	SARS-CoV-2	74.13 aM	Fluorescence	60 min	53
LwaCas13a	Endonuclease cycle amplification	sja-miR-2c5p	83.2 fM	Magnetic upconversion nanoparticles (MUCNPs) as a biosensor	60 min	54
Cas13a	DNAzyme-mediated signal amplification	miRNA-21	27 fM	Colorimetry	30 min	55
Cas13a	Entropy-driven cyclic amplification strategy	SARS-CoV-2	7.39 aM	Electrochemiluminescence (ECL)	80 min	56
Cas13a	T7	circRNA, miRNA, piRNA, and 16S rRNA	1.65 aM	QD-based FRET nano sensor	60 min	34
Cas13a	Rolling circle transcription (RCT)	piR-hsa-14	3.32 fM	Flour-plate reader	70 min	57
LwaCas13a	Transcription mediated amplification (TMA)	*P. jirovecii*-mitochondrial large subunit ribosomal RNA	2 copies per μL	Fluorescence	60 min	58
Cas13a	$Mn/NiCo_2O_4$ nanozyme as a signal amplifier	miRNA-143	Tens of aM	Colorimetric and fluorometric	60 min	59
Cas13a	Exo-III activity on the Ag^+-aptamer	miRNA-155	5.12 fM	Colorimetry	75 min	37
Cas13a	No	miRNA-21	10 aM	Fluorescence	60 min	40
Cas13a	No	*E. coli*, bacterial RNA	0.65 fM	Electrochemiluminescence, bipolar electrode-ECL lateral flow chip	20 min	60
LwaCas13a	No	SARS-CoV-2	100 aM	Capillary sensor (RNA-cross-linking DNA hydrogel film)	30 min	61
Cas13a	No	SARS-CoV-2	10 fM	Fluorescence	60 min	62
LwaCas13a	No	Synthetic RNA, pseudovirus	100 fM	On-chip total internal reflection fluorescence microscopy	~45 min	63

Table 1 (*continued*)

Type of enzyme	Preamplification	Target	LOD	Read out	Rxn time	Ref.
Cas13a	No	miRNA-21	9 fM	Photoelectrochemical (PEC) biosensing platform	60 min	64
Cas13a	No	Enterovirus B, Lassa, dengue, influenza A	1010 copies per μL	Fluorescence	—	65
Cas13a	No	Human circular RNA	0.089 fM	Electrochemical biosensor	~ 10 min	66
LbCas13a	No	SARS-CoV-2	2 aM	Fluorescence	15 min	39
LwCas13a	No	*Y. pestis*, *F. tularensis*, *Chlamydia psittaci*, *B. mallei*, *B. pseudomallei*, and *Brucella melitensis*	1 pM	FAM-RNA-MB electrochemical signal probe	25 min	67
LwCas13a	No	SARS-CoV-2	26.2 and 53.5 copies per μL	Electrochemical biosensor	200 min	68
LwaCas13a	No	Ebola RNA	291 aM	Fluorescence	40 min	69
LbuCas13a	No	SARS-CoV-2	10 aM	Fluorescence, digital droplets	~ 10–20 min	70
LbuCas13a	No	miRNA-21	75 aM	Fluorescent	30 min	71
LwCas13a	No	SARS-CoV-2	~ 200 copies per sample	Lateral-flow assay (LFA)	2 min lateral flow plus SHERLOCK	72
Cas13a	No	lncRNA H19	—	Fluorescence	—	73
6× His-twinstrep-SUMO-huLwCas13a	Light-triggered exponential amplification, RCA	miRNA-21	1 fM	ssDNA reporter with photocleavable linker	80 min	38
Cas13a–Cas12	Cas13a–12a amplification	miRNA-155	0.35 fM	Fluorescence	75 min	35
Hybrid Cas12a and Cas13a with SpyTag–SpyCatcher	RT-RPA	SARS-CoV-2	10 copies per reaction tube	Fluorescence		74

becomes activated and cleaves the RNA aptamer, disrupting its structure and suppressing fluorescence. This fluorescent change, detectable under UV light, offers a simple and equipment-free readout. Impressively, the system achieved detection of as few as 4 copies of the target RNA within 40 minutes.

Taking a different approach to amplify, Yan Sheng and colleagues (2021)[33] developed a reusable electrochemical biosensor that combines Cas13a with a catalytic hairpin DNA circuit (CHDC) (Fig. 3c). After Cas13a is activated by a target RNA, it initiates the CHDC, an enzyme-free signal amplification mechanism made up of two DNA hairpins. The first hairpin undergoes structural changes upon hybridizing with a nucleic acid trigger, while the second hairpin displaces the initial trigger in a strand-exchange reaction. Multiple cycles of hybridization process amplify the detection signal, which is then observed by an integrated screen-printed electrode chip. The detection, performed using square-wave voltammetry, achieves a LOD of 50 aM with a total process time of 36 minutes, highlighting the potential for low-cost, reusable, and highly sensitive RNA diagnostics.

Researchers have also identified additional preamplification strategies that offer unique advantages to enhance signal amplification further and broaden diagnostic applicability. One such method further refines sensitivity through a transcription-driven amplification mechanism. In a 2024 study, Wenjing Liu and colleagues introduced a nanosensor system that couples Cas13a with quantum dot (QD)-based fluorescence readout (Table 1). Upon target RNA recognition, Cas13a cleaves a substrate probe that subsequently serves as a promoter for T7 RNA polymerase. The resulting RNA transcripts are amplified and hybridized with both biotinylated capture probes and Cy5-labeled reporter probes anchored to a single QD.[34] This proximity facilitates fluorescence resonance energy transfer (FRET) between the QD and Cy5, generating a detectable signal with remarkable sensitivity—achieving a LOD of 1.65 aM in 60 minutes. The strategy elegantly combines enzymatic signal amplification with nanotechnology to offer precise detection in complex clinical samples, such as breast cancer tissue.

In a complementary direction, Dan Zhao *et al.* (2023)[35] introduced a dual-enzyme platform that integrates Cas13a with Cas12a in a sequential activation cascade (Fig. 3f). In this system, the target RNA activates Cas13a, which then cleaves a bulge structure within a blocker strand immobilized on magnetic beads. This cleavage event releases a primer strand that subsequently activates Cas12a. Once triggered, Cas12a initiates its well-known *trans*-cleavage activity, cutting a fluorescent ssDNA reporter and producing a measurable signal. This elegant two-stage mechanism enhances the detection sensitivity by combing two CRISPR activities, enabling signal amplification while maintaining sequence specificity. It exemplifies how multiple Cas systems can be strategically combined to maximize diagnostic performance.

Another creative use of amplification comes from the work of Jingjing Zhang *et al.* (2023),[36] who merged Cas13a activity with a branched hybridization chain reaction (bHCR) (Table 1). In this system, Cas13a's *trans*-cleavage is used to initiate the

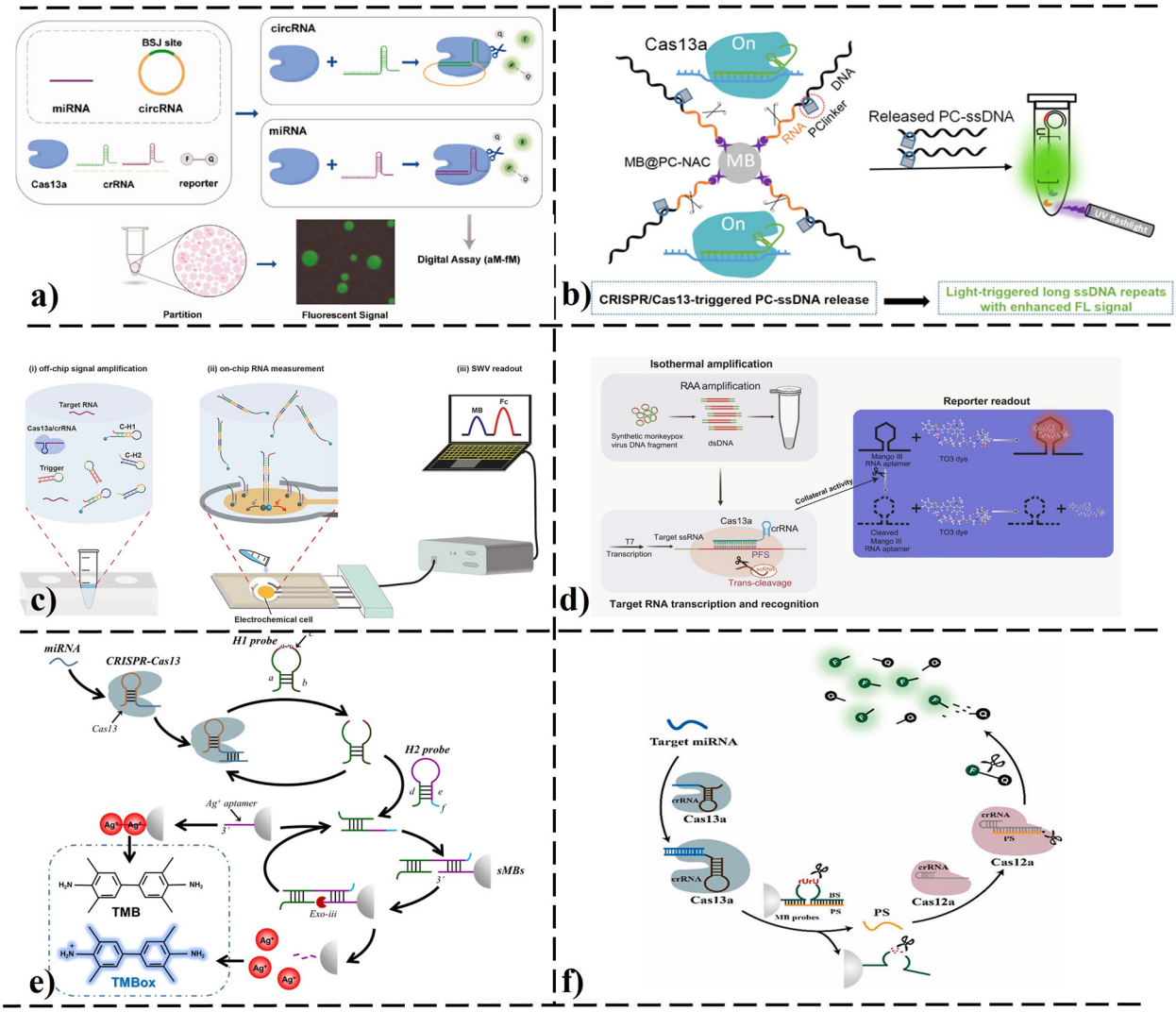

Fig. 3 (a) Schematic illustrating detection of RNA target using PddCas13a.[40] (b) Schematic of Cas13-triggered PC-ssDNA release from the MB@PC-NAC, padlock generation and under UV light and RCA amplification.[38] (c) Cas-CHDC-powered electrochemical RNA-sensing technology (COMET) chip: off-chip signal amplification (i), on-chip RNA measurements (ii), and square wave voltammetry (SWV) readout (iii).[33] (d) Schematic illustrating detection with RAA-Cas13a-Apt system.[32] (e) Schematic illustrating RNA detection using CRISPR/Cas13a-triggered exonuclease-iii-assisted colorimetric assay.[37] (f) Schematic illustration of Cas13a–12a amplification fluorescence biosensing platform.[35] Pdd: polydisperse droplet digital; PC: photocleavable linker; MB: methylene blue; PC-NAC: photocleavable linker-nucleic acid probe; RCA: rolling circle amplification; CHDC: catalytic hairpin DNA circuit; RAA: recombinase-aided amplification; Apt: aptamer.

bHCR by cleaving an RNA substrate that releases an initiator. This initiator then hybridizes to a DNA hairpin, triggering a chain reaction where subsequent hairpins unfold and extend the signal cascade. The resulting branched DNA structures are then detected using a surface-enhanced Raman scattering (SERS) sensor composed of silver nanorods. This method achieved a detection limit of 8.55 aM within 60 minutes, offering not only high sensitivity but also compatibility with SERS-based biosensing for label-free, multiplex-capable detection.

Building on these innovative signal amplification designs, Yunxiao Li *et al.* (2024)[37] introduced an exonuclease-III (Exo-III)-assisted Cas13a detection platform, integrating a clever aptamer-based reporting mechanism (Fig. 3e). Here, target activation triggers Cas13a to cleave a structured probe, releasing an intermediate strand that unlocks a silver ion (Ag^+)-binding aptamer. This structural change forms a protruding 3′-terminus, which is specifically recognized and cleaved by Exo-III, releasing Ag^+ ions. The liberated silver ions are then chelated again by excess aptamer, generating a visible color change. This multi-step cascade achieved a detection limit of 5.12 fM in around 110 minutes, demonstrating the effectiveness of integrating enzymatic cleavage and metal-ion signaling into CRISPR diagnostics.

Taking signal amplification a step further, Tao Hu *et al.* (2023)[38] presented a light-triggered system combining Cas13a and rolling circle amplification (RCA) (Fig. 3b). Upon target binding, Cas13a cleaves RNA substrates embedded in a photocleavable complex, enabling the light-controlled release of short DNA oligos with 5′ phosphate ends. These oligos serve

as triggers for RCA, generating long ssDNA products that emit strong fluorescence signals. This system achieves an excellent detection limit of 1 fM for RNA targets in 80 minutes.

1.2. Preamplification-free RNA detection. Cas13a has also been effectively used in systems that do not require preamplification and instead rely only on its inherent enzymatic activity. Many of these approaches capitalize on fluorescence-based readouts, where signal generation is directly linked to Cas13a's collateral cleavage once the target RNA is recognized.

One such example is described by Dou Wang (2023),[39] who developed a digital detection platform using magnetic beads to enrich and capture RNA targets (Table 1). Upon recognition, the Cas13a–crRNA complex initiates cleavage of a reporter molecule. The cleavage products are then compartmentalized into a femtoliter-scale microwell array, allowing individual fluorescent events to be resolved and quantified digitally. This digital assay approach minimizes background noise and supports highly sensitive detection.

A different but equally elegant strategy was proposed by Ke Wang *et al.* (2025)[40] through the development of polydisperse droplet digital (Pdd) Cas13a, a system utilizing polydisperse water-in-oil droplets as independent reaction chambers (Fig. 3a). In this setup, RNA molecules—including noncoding RNAs relevant to cancer—are randomly partitioned into thousands of droplets. Following incubation, only those droplets that contain target RNA activate Cas13a and emit a fluorescent signal. After 60 minutes, the droplets can be visualized under a fluorescence microscope, achieving a remarkable LOD as low as 10 aM. By combining microfluidics with Cas13-based collateral cleavage, this droplet system provides a scalable and precise method for digital RNA quantification without amplification.

2. RNA detection using CRISPR–Cas12

CRISPR–Cas12 enzymes, part of the type V CRISPR–Cas systems, have attracted increasing attention in the field of molecular diagnostics due to their robust and programmable collateral cleavage activity. Among the 11 known subtypes of CRISPR–Cas12 (Cas12a–u), only a subset—Cas12a (V-A), Cas12b (V-B), Cas12g (V-G), and more recently Cas12j (also known as CasΦ), has been utilized in RNA detection platforms (Table 2).[26,75] However, these enzymes differ in their mechanisms of RNA sensing. Cas12a, Cas12b, and Cas12j are inherently DNA-targeting nucleases, meaning they require the target RNA to be first reverse transcribed into complementary DNA (cDNA) before detection. In these systems, the detection is typically coupled with preamplification methods such as RT-RPA or RT-LAMP to generate DNA substrates that activate Cas12-mediated collateral cleavage. In contrast, Cas12g stands out as a unique subtype with the intrinsic ability to directly bind and cleave single-stranded RNA (ssRNA) targets, eliminating the need for reverse transcription or DNA intermediates.[76] This feature makes Cas12g a particularly attractive tool for streamlined and rapid RNA diagnostics. The following sections detail the use of each Cas12 subtype in RNA detection, with a focus on the preamplification techniques applied to identify various RNA targets.

2.1. RNA detection using CRISPR–Cas12a

2.1.1. Preamplification-based RNA detection. CRISPR–Cas12a has been widely employed for nucleic acid diagnostics across a variety of amplification strategies. These strategies can be broadly categorized into non-isothermal and isothermal methods, each with their own advantages and use cases.

2.1.1.1. Non-isothermal (PCR-based) methods. One of the earliest and most influential PCR–Cas12a platforms is the HOLMES system (one-hour low-cost multipurpose highly efficient system), developed by Li *et al.* (2018). This platform demonstrated Cas12a's utility in nucleic acid detection by leveraging its robust collateral cleavage activity. Although HOLMES is primarily a DNA detection system, it can also detect RNA targets by incorporating an initial reverse transcription (RT) step to convert RNA into cDNA. HOLMES also showcased the ability to distinguish single-nucleotide polymorphisms (SNPs) by modifying the protospacer adjacent motif (PAM) region or adjusting the crRNA guide sequence, with shorter guide RNAs enhancing specificity.[77]

Building on this, Ning *et al.* (2022) applied a Cas12a-based platform to detect RNA variants, again using reverse transcription by either RT-PCR or RT-RPA to generate DNA amplicons as targets for Cas12a detection. Notably, their system could discriminate between different viral variants by targeting mutations within the PAM or seed region and showed potential for smartphone-based POC diagnostics.[78]

2.1.1.2. Isothermal methods. While PCR-based amplification has long been the gold standard for nucleic acid detection, its reliance on thermal cycling limits its utility in low-resource and POC settings. By combining the specific collateral cleavage activity of Cas12a with various isothermal preamplification strategies, such as RPA, LAMP, RAA, RCA, and others, new diagnostic platforms have emerged that achieve high sensitivity and specificity without the need for complex thermal cycling equipment. Among these strategies, reverse transcription-recombinase polymerase amplification (RT-RPA) has proven particularly effective, enabling rapid RNA-to-DNA conversion and amplification under simple conditions. By integrating RT-RPA with Cas12a, the Crispr diagnostic platform enhanced fluorescence signal strength dramatically, making results detectable even with a cell phone (Fig. 4a). This not only boosted sensitivity but also pushed CRISPR diagnostics closer to true portability.[79]

Building on the momentum of RPA, researchers also explored loop-mediated isothermal amplification (RT-LAMP) as a complementary strategy. Unlike multi-step processes, LAMP allowed amplification and Cas12a-mediated detection to occur in a single vessel, reducing contamination risks (Fig. 4c).[80] Systems like opvCRISPR exemplified this streamlined design, achieving near single-molecule detection sensitivity and offering simple visual readouts, making sophisticated molecular diagnostics accessible beyond laboratory environments.[81] As efforts continued to refine speed and field applicability, recombinase-aided amplification (RT-RAA) emerged as another promising technique (Fig. 4e).[82] Its low-temperature

Table 2 CRISPR–Cas12-based RNA detection methods integrated with various preamplification strategies

Type of enzyme	Preamplification	Target RNA	LOD	Read out	Rxn time	Ref.
Cas12a	PCR	Infected cell culture	aM	Fluorescence	~1 h	77
Cas12a	RT-PCR	SARS-CoV-2	0.5 copies per mL	Fluorescence	110 minutes	78
Cas12a	RT-LAMP	SARS-CoV-2	5 copies	Fluorescent detection by naked eye under blue light		81
LbCas12a	LAMP	RNAseP POP7 mRNA	16 copies per μL	—	110 minutes	109
Cas12a	RPA/RT-RPA	Ebola virus	11 aM	μPAD readout	1–4 h	110
Cas12a	RPA	HRSV	100 copies per mL	Fluorescence	60 minutes	111
Cas12a	RPA	HIV	200 copies per test	Glucose meter	~70 minutes	112
AsCas12a, LbCas12a	RPA/RT-RPA	Rice black-streaked dwarf virus (RBSDV)	1 aM	Lateral flow and fluorescence	30–60 minutes	49
Cas12a	RT-RPA	Potato virus X (PVX), and potato virus Y (PVY)	fM levels	Fluorescence	~20 minutes	113
Cas12a	RT-RPA	Conserved fragments within the VP2 gene of the norovirus GII.2 subtype	10 copies per μL	Lateral flow	25–35 minutes	114
LbCas12a	RPA/RT-RPA	Apple necrotic mosaic virus (ApNMV), apple stem pitting virus (ASPV), apple stem grooving virus (ASGV), apple chlorotic leaf spot virus (ACLSV) and apple scar skin viroid (ASSVd)	25 viral copies per reaction	Oligonucleotide-conjugated gold nanoparticles	~50 minutes	115
LbCas12a	RPA/RT-RPA	microRNAs	~aM	G-quadruplex (G4) containing a hairpin structure as the reporter	1 hour preamplification + 40 minutes CRISPR rxn	116
Cas12a	RPA	miRNA-21	3.43 aM	Fluorescence	40 min preamplification + 30 min cleavage reaction	117
Cas12a	RPA/RT-RPA	SARS-CoV-2	0.38 copies per μL	Fluorescence detection using a smartphone-based device	15 minutes	79
SuCas12a2	RPA	Transcripts of the EhPrx and p1 genes	10^2 copies per reaction	Fluorescence	40 min preamplification + 45 min cleavage reaction	118
MeCas12a (manganese-enhanced Cas12a)	RT-RAA	MERS-CoV	5 copies	Fluorescence	~45 min	82
Cas12a	RT-RAA	SARS-CoV-2	1 copy per μL	Fluorescence	15 min preamplification + 10 min cleavage reaction	119
Cas12a	RCA	SARS-CoV-2	604 fM	Portable glucose meter (PGM)	3 h	120
Cas12a	RCA	miRNAs	0.52 aM	Electrochemical	~4 h	121
Cas12a	RCA	miRNA-21	16 aM	Chemiluminescence (CL)	~4 h	122
Cas12a	Hyperbranched rolling circle amplification (HRCA)	miRNA-21	10.02 fM	Fluorescence	223 min preamplification + 50 min cleavage reaction	123
LbCas12a	HRCA	miRNA-143	1 fM	Gold nanoparticle (AuNP)-based visual assay	45–50 minutes	124
Cas12a	Branched rolling circle amplification (BRCA)	Primers incorporating ncRNA sequences	12 pM	Fluorescence	One hour	125

Table 2 (*continued*)

Type of enzyme	Preamplification	Target RNA	LOD	Read out	Rxn time	Ref.
		of circulating CRC-associated RNAs (piRNA)				
FnCas12a	Multiply-primed rolling circle amplification (MRCA)	SARS-CoV-2	1.625 copies per reaction	Lateral flow and fluorescence	20 to 60 minutes	83
Cas12a	3D DNA walker cascade amplification	miRNA-214	20.42 fM	Fluorescence		126
LbCas12a	3D DNA walker cascade amplification	miRNA-141	0.331 fM	Electrochemiluminescence (ECL)	1 day and a few hours	127
Cas12a	Reverse transcription-free exponential amplification reaction (RTF-EXPAR)	SARS-CoV-2	3.77 aM	Fluorescence	40 minutes	128
Cas12a	EXPAR	miRNA-21	3.2 fM	Electrochemical	80 minutes preamplification + 40 minutes cleavage reaction	85
Cas12a	EXPAR	miRNA-155	85 aM	Dual-channel fluorescence and colorimetric signal output	80 minutes preamplification + 20 minutes cleavage reaction	84
LbCas12a	CHA	miRNAs	∼100 fM	ECL	2 hours	129
LbCas12a	CHA	miRNA-122	2.04 fM	Photoelectrochemical (PEC) biosensor	3 hours preamplification + 1 hour cleavage reaction	130
LbCas12a	CHA	miRNA-21	0.48 fM	ECL	—	131
LbCas12a	CHA	miR-128-3p	2.5 to 8.98 fM	Fluorescence	75 minutes preamplification + 60 minutes cleavage reaction	87
Cas12a	HCR	miRNA-141	3.3 fM	ECL	3 hours preamplification + 1 hour cleavage reaction	132
LbCas12a	HCR	miRNA-21	75.4 aM	Fluorescence	2 hours preamplification + 8 minutes cleavage reaction	86
Cas12a	T7 RNA polymerase	miRNAs	1 pM	Fluorescence	160 minutes preamplification + 150 minutes cleavage reaction	89
FnCas12a	RT-HDA	Deformed wing virus (DWV) RNA	500 fM	Fluorescence	90 minutes preamplification + 45 minutes cleavage reaction	133
AsCas12a	HDA	SARS-CoV-2, SCGB2A2 (mammaglobin A) RNA	0.6 copies per μL	Lateral flow and fluorescence	90 minutes	92
Cas12a	Target-induced transcription process *via* split-T7 promoter	miRNA-21 isothermal amplification	43.9 fM	Fluorescence	∼1 h	134
Cas12a	RCA + CHE	Rabies viral RNA	2.8 pM	ECL	∼11 h	135
Cas12a	RCA + CHA	microRNA-320d	0.342 fM	ECL	3 hours RCA + 3 hours CHA + 2 hours Cas12a rxn	136
Cas12a	Dual-signal amplification (Exo III amplification + RCA)	miRNA-21	6.01 fM	Fluorescence	5.5 hours	137
LbCas12a	Strand displacement reaction (SDR)	miRNA-21	2.42 fM	Fluorescence	∼4 h	88
Cas12a	Toehold-mediated strand displacement reaction (TSDR)	SARS-CoV-2	40 aM	Electrochemical	90 minutes preamplification + 40 minutes cleavage reaction	138
Cas12a	Entropy-driven catalysis (EDC) cycle amplification	miRNA-21	1.5 fM	PEC	∼4 h	90
Cas12a	Strand displacement amplification (SDA)	miRNA-let-7a	6.28 pM	Distance-based biosensor	1 hours preamplification + 30 minutes cleavage reaction	139
Cas12a	SDA	miRNA-21	0.5 fM	Single-particle inductively coupled plasma-mass spectrometry	2 hours and 15 minutes	91
Cas12a	Self-primer-initiated (SPI)-CRISPR–Cas12a-assisted amplification	miRNAs	254 aM	Functionalized gold nanoparticle (AuNP)-based color generation	60 minutes preamplification + 30 minutes cleavage reaction	140
Cas12a	T7 exonuclease-assisted target recycling	bacterial 16S rRNA (rRNA)	3.6 pM	Split G-quadruplex (G4) catalytic signal output	—	141
Cas12a	—	DENV	100 fM	Electrochemical	∼30 min	142
Cas12a	—	HCV RNA, miRNA-155	767 pM	Fluorescence	1 h	98
Cas12a	—	SARS-CoV-2	50 copies per μL	Fluorescence	∼71 min	93

Table 2 (*continued*)

Type of enzyme	Preamplification	Target RNA	LOD	Read out	Rxn time	Ref.
Cas12a	—	SARS-CoV-2	50 copies per μL	PGM	—	94
Cas12a	—	SARS-CoV-2	10 fM	Fluorescence	30 minutes	101
Cas12a	—	miRNA-21	10 fM	Fluorescence	5 minutes	96
Cas12a	—	SARS-CoV-2	2.2 pM	Fluorescence	45 minutes	95
Cas12a	—	miRNA-21	301 fM	Lateral flow assay	60 minutes	143
Cas12a	—	miRNA-19a	856 aM	Fluorescence	20 minutes	99
Cas12a	—	miRNA-10b	5.53 fM	Reverse fluorescence-enhanced lateral flow test strip (rFLTS)	40 minutes	144
Cas12a	—	miRNA-21	10 pM	Lateral flow and fluorescence	30 minutes	102
Cas12b	RT-LAMP	SARS-CoV-2, human adenovirus, herpes simplex virus	1 copy per μl	Fluorescence	—	105
eBrCas12b	RT-LAMP	HCV	—	Fluorescence	∼1 h	103
Cas12b	LAMP	mRNAs	10^{-8} nM	Fluorescence	—	145
AapCas12b	LAMP	SARS-CoV-2	10 copies per reaction	Lateral flow and fluorescence	—	146
AapCas12b	RT-RPA	SARS-CoV-2	8 copies per μL	Fluorescence	30 to 60 minutes	106
BhCas12b	No	CJ8421_04975 mRNA from *Campylobacter jejuni*	1 μM	Fluorescence	45 min	147
Cas12j	EXPAR	miRNA-92a, miRNA-122, and miRNA-155	3.2 fM	Fluorescence	30 minutes	107
Cas12g	PCR	—	—	Gel electrophoresis	30 minutes	76
Cas12g	—	—	—	Running the reaction samples on 20% PAGE TBE-urea denaturing gels stained with GelRed nucleic acid gel stain, and the results were visualized using alpha innotech (fluouchem TM)	—	108
Cas12g1	—	—	100–125 pM	Gel electrophoresis	—	148

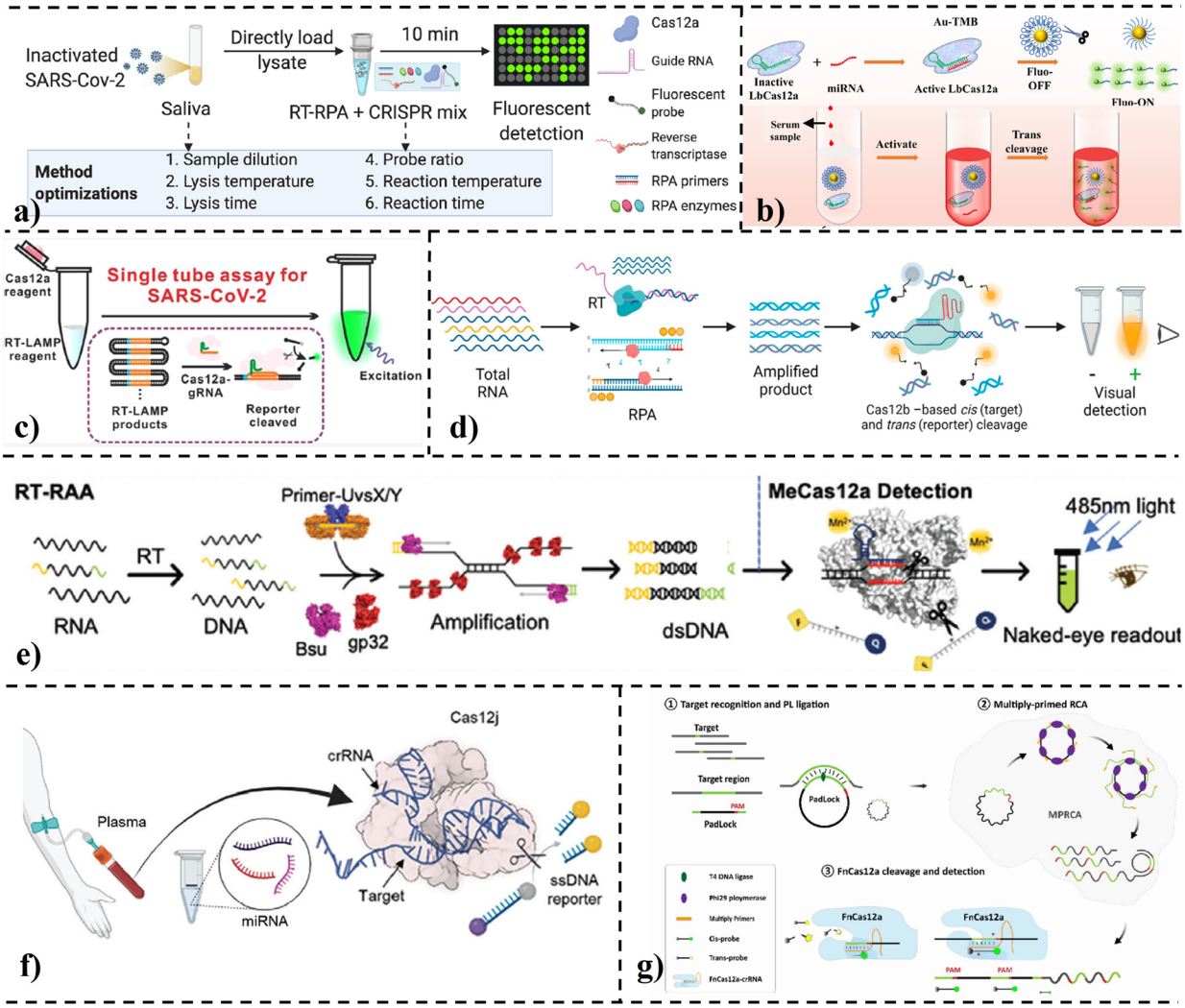

Fig. 4 (a) CRISPR–FDS assay optimization using spiked saliva samples. Steps 1–3 tested different lysis buffer dilutions to enhance RNA release and fluorescence detection.[79] (b) Schematic showing CRISPR/LbCas12a *trans*-cleavage activity on gold nanoparticles (AuNPs) for direct RNA detection.[96] (c) Schematic illustrating the core principle and overall workflow of the RT-LAMP and Cas12a-based RNA detection assay.[80] (d) Schematic of iSCAN-V2: a one-tube assay combining reverse transcription, amplification, and Cas12b-mediated collateral cleavage for fluorescent RNA detection from swab samples.[106] (e) The process of viral RNA detection using reverse transcription recombinase-aided amplification (RT-RAA) combined with MeCas12a-based detection.[82] (f) Workflow of the EXP-J reaction for lung cancer diagnosis.[107] (g) Demonstration of the enzyme-catalyzed rolling circle amplification-assisted CRISPR/FnCas12a assay through stepwise reactions, with a conceptual diagram illustrating the padlock probe and PAM-free design.[83] RT-LAMP: reverse transcription loop-mediated isothermal amplification; iSCAN: *in vitro* specific CRISPR-based assay for nucleic acids; RT-RAA: reverse transcription recombinase-aided amplification; EXP-J: exponential junction (EXP-junction) amplification.

operation and rapid amplification kinetics made it ideal for time-critical diagnostics. When integrated into a centrifugal microfluidic platform, RT-RAA combined with Cas12a achieved detection of viral RNA at single-copy sensitivity within 30 minutes, with diagnostic accuracy matching that of RT-PCR. This demonstrated that high performance could be maintained even in settings where complex equipment is impractical.

While many platforms focused on cDNA intermediates, others sought to simplify the workflow further by bypassing reverse transcription altogether. Rolling circle amplification (RCA) provided such an opportunity. RCA-based systems like OPERATOR[83] used RNA-templated DNA ligation to initiate multiply-primed amplification, producing products that directly activated Cas12a without prior cDNA synthesis (Fig. 4g). Ingenious variations like CRISPR–PGM even converted nucleic acid detection into glucose readouts measurable by handheld meters, illustrating how CRISPR and RCA could be combined for affordable, decentralized diagnostics.[83]

In pursuit of even faster and more sensitive assays, researchers turned to an exponential amplification reaction (EXPAR). EXPAR has emerged as a powerful partner to Cas12a in RNA diagnostics, offering rapid, highly sensitive, and versatile detection. By leveraging EXPAR's strong amplification capability alongside Cas12a's collateral cleavage activity, several studies have demonstrated detection of miRNAs and viral RNAs at femtomolar to attomolar concentrations.[84] One key advantage

of this approach is the high specificity achieved through Cas12a's sequence-specific recognition, which significantly reduces false positives often associated with isothermal amplification alone. Additionally, multiplex detection has been demonstrated using EXPAR-generated dual ssDNA triggers to activate Cas12a in an "AND" logic circuit, enabling the simultaneous detection of multiple miRNA targets with a single crRNA complex. EXPAR–Cas12a platforms have also introduced dual-mode signal outputs (*e.g.*, fluorescence and colorimetric readouts), increasing result reliability and flexibility. Smartphone integration for POC testing (POCT) has further enhanced the portability and accessibility of these systems.[85]

Alongside these enzyme-driven amplifications, catalytic hairpin assembly (CHA) offered a simpler, enzyme-free alternative. Integrating CHA with Cas12a enabled one-step, highly sensitive RNA detection, sidestepping multiple handling steps and reducing contamination risk. Creative adaptations pushed detection sensitivity into the femtomolar range, while combination strategies involving photoelectrochemical and electrochemiluminescence methods enhanced signal clarity and minimized background noise. Notably, platforms like MCM-CRISPR/Cas12a, combining CHA with hybridization chain reaction (HCR),[86] demonstrated detection of low-abundance non-coding RNAs with remarkable precision.[87]

Beyond the major amplification strategies discussed, other methods such as hybridization chain reaction (HCR),[86] strand displacement reaction (SDR),[88] binding-induced primer-triggered cascade (BPTC),[89] enzyme-driven cascade amplification (EDC),[90] and strand displacement amplification (SDA)[91] have also been employed in Cas12a-based RNA detection. Though less commonly used, these approaches provide valuable enhancements in sensitivity, specificity, or workflow flexibility. Among these, one particularly notable system combined SDA with Cas12a and utilized single-particle inductively coupled plasma mass spectrometry (spICP-MS) for detection. This platform integrated SDA with Cas12a *trans*-cleavage and employed gold nanoparticle labels to achieve a quantification limit of 0.5 aM. With a 45-minute reaction time, this system offers an optimal balance of sensitivity and detection kinetics for clinical applications.[91] Another innovative approach is the flap endonuclease, Taq ligase and CRISPR–Cas for diagnostics (X) (FELICX) platform, which uniquely uses flap endonuclease (FEN) for target recognition, enabling PAM-independent detection. This is followed by adaptor ligation and Cas12a activation, and when combined with RTx-HDA, FELICX achieved RNA detection at 1 aM sensitivity within 90 minutes. Its independence from guide RNA optimization and compatibility with both DNA and RNA targets make FELICX an exceptionally versatile and practical platform for molecular diagnostics.[92]

2.1.2. *Preamplification-free methods*

2.1.2.1. Use of complete crRNA and complete activator. While many CRISPR/Cas12a-based platforms rely on nucleic acid preamplification to enhance sensitivity, several studies have developed strategies that enable RNA detection without preamplification. These amplification-free systems still harness the collateral cleavage activity of Cas12a, but differ in how they handle the RNA target, particularly in their requirements for reverse transcription and activation mechanisms. One major class within these approaches involves the use of a complete crRNA and a complete activator, preserving the canonical structure of the Cas12a system without splitting either component.

In some of these systems, although the detection phase is preamplification-free, the RNA target is first reverse transcribed into cDNA before Cas12a engagement which is due to the intrinsic nature of Cas12a that will be activated by DNA targets. In one such example, viral RNA was reverse transcribed using a gene-specific primer and a commercial reverse transcription kit. The resulting cDNA acted as a trigger for Cas12a, allowing the detection step to proceed without preamplification. This system maintained high sensitivity, reaching detection limits in the femtomolar range, despite skipping the preamplification phase.[93] Another approach under the same category departs from direct activation of Cas12a by instead employing the RNA as a competitive inhibitor. In this method, Cas12a is initially activated by a target DNA sequence (tcDNA), which triggers its nonspecific ssDNA cleavage activity. When the target RNA is present, it competes with the DNA activator for binding to the crRNA–Cas12a complex, effectively suppressing Cas12a's *trans*-cleavage function. This change in enzymatic behaviour is then monitored electrochemically. Unlike the previous example, this system does not require reverse transcription, relying instead on RNA's ability to modulate Cas12a activity through competitive inhibition. This approach maintains an amplification-free and label-free detection process and reveals a different dimension of Cas12a's programmability, where signal generation can occur through inhibition rather than activation.[94]

Progressing further within the same category, recent studies have shown that Cas12a can, under certain optimized conditions, be directly activated by RNA targets, challenging the previous assumption that Cas12a only responds to DNA triggers. In one such example, functionalized magnetic beads were employed to capture the target RNA alongside signal probes containing activation sequences for Cas12a. Once bound, magnetic separation isolated the RNA-probe complex, and the addition of Cas12a and crRNA allowed the probe itself to activate Cas12a, leading to collateral cleavage of fluorescent reporters. Notably, the use of manganese ions in place of magnesium was found to enhance Cas12a's cleavage efficiency, enabling RNA detection with high precision in clinical settings, all without preamplification or reverse transcription. This technique delivered results within 45 minutes with a detection limit of 2.2 pM.[95]

In a parallel strategy, another group introduced a nanomaterial-enhanced system, where gold nanoparticle-based nanobeacons (Au-nanobeacons) were used as reporters. In this case, Cas12a's collateral activity was directly triggered by RNA, specifically miRNA, without any DNA intermediates or pretreatment. The Au-nanobeacons offered both faster kinetics and enhanced sensitivity compared to traditional fluorescent reporters. With a detection limit reaching as low as 10 fM in just five minutes of reaction, and validated performance in

serum, this method pushes the boundaries of what Cas12a can achieve in its unamplified, native state (Fig. 4b).[96] In addition, a recent crRNA spacer regulation-based SCas12aV2 assay demonstrated robust and programmable Cas12a activation by leveraging stem–loop-structured crRNAs, enabling sensitive and modular detection of structured RNA targets, including SARS-CoV-2, miRNAs, and circRNAs, with high specificity and one-pot isothermal readout capability.[97]

2.1.2.2. Use of complete crRNA and split activator. Expanding on amplification-free strategies, a distinct class of RNA detection methods uses complete crRNA while employing split activators to initiate Cas12a *trans*-cleavage activity. A key advancement in this category was demonstrated by the SAHARA method, which revealed that while Cas12a requires DNA at the PAM-proximal seed region for activation, the PAM-distal region of the crRNA can interact with RNA. By supplying a short DNA oligonucleotide to occupy the seed region and using the RNA target to complement the distal part of crRNA, this method enables direct RNA detection without reverse transcription or preamplification.[98]

A separate yet related method employed a competitive displacement mechanism for signal enhancement. This technique utilized both a full-length crRNA and a split crRNA that compete for Cas12a binding. Initially, the full crRNA activates Cas12a upon binding to the RNA, triggering *trans*-cleavage. Subsequently, the split crRNA replaces the full one, initiating a secondary round of activation—thus creating a cascade signal amplification. While still based on complete crRNA recognition of the RNA target, this approach enhances sensitivity by exploiting the dynamic binding interactions between full and split crRNAs.[99] More recently, a flexible ''splice-at-will'' crRNA engineering strategy was introduced, enabling precise and sensitive Cas12a-mediated detection of ultrashort RNAs (as short as 6–8 nt) by reconstituting functional crRNAs through modular hybridization at nearly any site within the spacer region using a DNA splint and target RNA.[100]

Together, these studies demonstrate how split activators, whether composed of synthetic DNA, endogenous RNA, or a combination can be paired with complete crRNA to create preamplification-free Cas12a systems. These systems elegantly bypass the need for reverse transcription by selectively engaging different regions of the crRNA with engineered or native sequences, broadening the toolkit for rapid, sensitive, and versatile RNA diagnostics.

2.1.2.3. Use of split crRNA and complete activator. The third and most recent strategy in the realm of amplification-free Cas12a-based RNA detection introduces a fundamentally different design: split crRNA systems paired with a complete activator. In these approaches, the standard crRNA is intentionally divided into two or more RNA fragments, each alone insufficient to activate Cas12a. However, when brought into close proximity by an activator or target molecule, these fragments reassemble into a functional guide, enabling controlled and highly specific RNA sensing.

A notable example of this concept is the PARC–Cas12a platform (proximity-activated RNA-guided Cas12a), where the crRNA is split within its 5′ handle domain. In this system, activation of Cas12a is contingent on the reconstitution of the guide RNA, which occurs only when the split fragments are spatially brought together. This is achieved through the hybridization of the fragments to a shared trigger molecule, such as an RNA sequence, aptamer, or small molecule. This proximity-dependent assembly transforms Cas12a into a programmable biosensor, enabling logic-gated detection schemes and multiplexing. The system has also been successfully integrated into platforms like arrayPARC–Cas12a and ICP-MS-based assays, enhancing its diagnostic versatility.[101]

Another important contribution in this space is the development of SCas12a, a system that fully separates the scaffold RNA from the spacer RNA. Here, the target RNA, such as a mature miRNA, directly serves as the spacer component. In the presence of a complementary ssDNA activator and the scaffold RNA, the miRNA completes the crRNA assembly and triggers Cas12a's *trans*-cleavage activity. This method achieves direct RNA detection without preamplification or reverse transcription and does so with high sensitivity in the femtomolar range. Moreover, SCas12a exhibits strong discrimination power, capable of distinguishing closely related sequences, as well as single-nucleotide variants.[102]

2.2. RNA detection using Cas12b. Recent years have seen considerable progress in adapting Cas12b enzymes for RNA detection, especially by leveraging their compatibility with one-pot isothermal amplification strategies. Among these, RT-LAMP has been the most widely utilized due to its high efficiency and optimal temperature range aligning with engineered Cas12b activity.

A major advancement in this area came with the engineering of a thermostable Cas12b variant, BrCas12b, derived from *Brevibacillus* sp. and further optimized through hydrophobic core mutations to enhance its *trans*-cleavage activity at elevated temperatures. This engineered enzyme, eBrCas12b, retains robust performance up to 67 °C, allowing seamless integration with RT-LAMP reactions.[103] Utilizing this capability, the SPLENDID platform was developed, a single-pot LAMP-mediated detection assay clinically validated for RNA detection in human serum and saliva. The system demonstrated high specificity and accuracy, completing detection within one hour and outperforming standard RT-LAMP by significantly reducing false positives.[103] Similarly, the STOPCovid assay used AapCas12b from *Alicyclobacillus acidiphilus* in a one-pot RT-LAMP setup, optimized through guide RNA engineering and the addition of taurine to accelerate reaction kinetics.[104]

Moving beyond conventional detection, the WS-RADICA platform introduced a digital format for Cas12b-based diagnostics. Combining warm-start RT-LAMP with Cas12b in a droplet-based digital system, this method achieved a detection limit as low as 1 copy per μL, offering both qualitative and quantitative output. Notably, WS-RADICA performed well under challenging conditions, showing tolerance to common inhibitors like EDTA and SDS, and providing quantification

accuracy comparable to RT-qPCR and RT-dPCR, while offering faster results and broader application to both RNA and DNA viruses.[105]

In addition to RT-LAMP, RT-RPA has also been explored as a lower-temperature alternative. While less widely reported, some systems have demonstrated effective coupling of Cas12b with RT-RPA for rapid RNA detection, particularly when rapid deployment or reduced thermal requirements are needed. However, further engineering is typically required to adapt Cas12b's activity to RPA's temperature window. The iSCAN-V2 platform is another example of using RT-RPA, offering a one-pot, preamplification-based assay where Cas12b outperformed Cas12a in both signal strength and speed (Fig. 4d). The assay achieved a LOD of 8 copies per μL, and in clinical validation, it showed 93.75% sensitivity and 100% specificity, reliably detecting RNA in samples with cycle threshold (Ct) $\leq$ 30 in under an hour.[106]

Overall, Cas12b-based systems have rapidly evolved into highly sensitive, amplification-compatible diagnostic tools. Their thermal stability, compatibility with one-pot formats, and adaptability to digital platforms make them particularly promising for clinical, field-based, and POC RNA diagnostics, especially in settings requiring speed, specificity, and minimal equipment.

2.3. RNA detection using Cas12j. Cas12j, also known as CasΦ, represents a relatively new addition to the CRISPR–Cas family, and recent studies have begun to uncover its diagnostic potential. One significant advancement came from the work of Ju-Eun Kang, who demonstrated that Cas12j enzymes possess robust *trans*-cleavage activity suitable for nucleic acid detection. In particular, this study focused on detecting miRNA targets, which are often challenging due to their short length and low abundance. The researchers developed a method called EXP-J (exponential amplification reaction with Cas12j), which harnesses Cas12j's *trans*-cleavage activity to generate a fluorescent signal in response to target miRNAs (Fig. 4f). The system uses a two-part design: a converter and a repeater that together amplify a trigger DNA sequence (X) in the presence of the miRNA. This amplified trigger then activates Cas12j to cleave a fluorescent reporter, enabling sensitive detection. Three Cas12j variants, Cas12j1, Cas12j2, and Cas12j3, were tested, with Cas12j3 emerging as the most effective, showing the fastest signal response and the highest sensitivity. The method also proved to be highly specific, with signal generation observed only in the presence of the target miRNA. Furthermore, receiver operating characteristic (ROC) curve analysis revealed high diagnostic accuracy, confirming the assay's potential in clinical applications. Together, these findings highlight Cas12j3 as a promising enzyme for rapid, sensitive, and specific RNA detection, especially in the context of small RNA biomarkers like miRNAs.[107]

2.4. RNA detection using Cas12g. Among the Cas12 family, Cas12g stands out for its unique ability to function as an RNA-guided ribonuclease that directly targets single-stranded RNA (ssRNA). Unlike other Cas12 subtypes such as Cas12a, Cas12b, or Cas12e—which are primarily DNA-targeting enzymes, Cas12g operates more like a type VI effector, offering a natural platform for RNA-focused applications.[76]

Structural and biochemical analyses have confirmed Cas12g's capacity for RNA detection. It employs a dual-guide RNA system, a crRNA and a tracrRNA, or a fused single-guide RNA (sgRNA), to recognize RNA sequences with no requirement for a PAM or protospacer flanking sequence (PFS). This feature removes a major limitation in CRISPR targeting and simplifies assay design for RNA diagnostics. Importantly, studies have shown that Cas12g demonstrates comparable RNA detection sensitivity to top-performing Cas13 effectors, while maintaining thermostability, broadening its potential for both laboratory and POC applications.[108]

While no fully realized Cas12g-based diagnostic assay has yet been reported, recent cryo-EM and crystal structure analyses have provided critical insight into its molecular mechanism. These studies revealed Cas12g's bilobed architecture and highlighted key structural components, including the REC and NUC lobes, zinc finger motifs, and the lid motif within the RuvC domain, offering a blueprint for engineering future RNA detection platforms.[76,108]

3. RNA detection using CRISPR–Cas9

While Cas9 is widely known for its DNA-targeting capabilities, recent innovations have expanded its role into RNA detection, particularly by integrating it with preamplification strategies to enhance sensitivity (Table 3). One early approach, the Cas9 nickase-assisted isothermal amplification reaction (Cas9 nAR and its optimized version Cas9 nAR-v2), cleverly combines reverse transcription with strand displacement activity. Here, RNA is first transcribed into cDNA, and a rationally engineered Cas9 nickase introduces specific nicks that enable DNA polymerase to extend and amplify the target sequence under isothermal conditions, allowing rapid detection through fluorescence or lateral flow assays in a single reaction tube.[149] To build on this specificity without relying on fluorescent labels, researchers adapted catalytically inactive Cas9 (dCas9) into a biosensing platform coupled with surface plasmon resonance (SPR). In this system, amplified targets hybridize to primers immobilized on a sensor surface, and dCas9 binding creates significant refractive index changes, boosting the detection signal through a simple, label-free readout.[150]

Recognizing the need for even faster and more sensitive detection, other strategies combined Cas9 cleavage with exponential amplification reactions (CAS-EXPAR). After site-specific cleavage of DNA or cDNA by Cas9/sgRNA, short fragments are generated that trigger an EXPAR cascade, exponentially amplifying the signal for highly sensitive, real-time RNA detection.[151] The evolution toward digital detection led to the development of dCRISTOR, which uses dCas9-engineered magnetic micromotors. Following LAMP[152] amplification of RNA, the micromotors bind specific amplicons and change their motion when exposed to a magnetic field, allowing deep learning algorithms to digitally classify positive or negative detection events. Further innovations explored rolling circle amplification (RCA) paired with Cas9 systems. In the RACE method, a padlock probe is ligated to the target miRNA, generating a circular template that undergoes RCA to produce long ssDNA, which is then recognized

Table 3 RNA detection strategies employing CRISPR enzymes beyond Cas13 and Cas12 in combination with various preamplification methods

Type of enzyme	Preamplification	Target	LOD	Read out	Rxn time	Ref.
Cas10 subunit from the type III-A CRISPR complex	RT-LAMP	SARS-CoV-2	10^8 copies per reaction	Fluorometric + colorimetric detection	∼1 h	165
Cas10 subunit of the type III-B Cmr complex	RT-LAMP	SARS-CoV-2	800 aM	Fluorescence	180 minutes	166
Cas10 subunit within the type III-A CRISPR complex	—	SARS-CoV-2	10^6 copies per μL	Fluorescence, gel electrophoresis, thin-layer chromatography (TLC)	10 minutes	175
Cas10 subunit within the type III-B CRISPR complex	—	SARS-CoV-2	8 fM	Fluorescence	30–50 minutes	167
Cas10 subunit within the type III-A CRISPR complex	Isothermal amplification	SARS-CoV-2	aM	Fluorescence	—	176
Cas10	No	*T. congolense* 7SL-sRNA	10–100 fM	Lateral flow and fluorescence	∼2 h	168
Cas10 subunit of the *Staphylococcus epidermidis* Cas10–Csm complex	No	Target RNA	—	Denaturing PAGE and autoradiography	30–60 minutes	177
Cas10 subunit within various Csm complexes	No	Target RNA	—	Denaturing gel electrophoresis and autoradiography	Up to 120 minutes	170
Cas10 subunit of the *Lactobacillus delbrueckii* subsp.	No	miRNA-155	500 pM–2 nM	Fluorescence	30–60 minutes	169
Cas10 subunit of the *Sulfolobus tokodaii* Csm (StCsm) complex	No	SARS-CoV-2	—	Agarose gel electrophoresis with EB staining	60 minutes	178
Cas7–11	Rt-RPA	SARS-CoV-2	2 fM	Fluorescence	∼2 h	171
Type III-E Cas7–11	—	Various target RNAs	—	Fluorescence	—	172
Cas14a	EDC	miRNA-10b	2.1 pM	Fluorescence spectrophotometry	2 hours	159
Cas14a1	Asymmetric PCR	Bacterial RNAs (*Streptococcus pyogenes* and *Eberthella typhi*)	105 CFU per mL	Fluorescence	2 hours	162
Cas14a	RCA	miRNA156a from banana	1.839 pM	Fluorescence	2 hours	160
Cas14a	SDA	miRNA-21	680 fM	Fluorescence	1 hours	164
Cas14	RT-LAMP	RNA2 gene of the red-spotted grouper nervous necrosis virus (RGNNV)	63.4 aM	Fluorescence	2 hours	161
Cas14a	Toehold-containing three-way junction (TWJ)	RNA viruses	—	Magnetic separation enhanced colorimetry	—	179
Cas14 (AsCas12f1)	No	CJ8421_04975 mRNA from *Campylobacter jejuni*	—	Fluorescence	—	147
Cas14a1	Transcription by T7 RNA polymerase	16S rRNA of bacteria (specifically *E. typhi*)	0.6 aM	Fluorescence	1 hours	163
Pyrococcus furiosus (Pfu) Cas3	No	ssRNA target	0.1–1 nM	Fluorescence	15 minutes	180
E. coli Cas3	RT-LAMP	SARS-CoV-2	<102 copies	Lateral flow and fluorescence	32–42 minutes	173
fastCas9n (derived from *Streptococcus pyogenes* Cas9 (SpCas9))	—	*Salmonella typhimurium* 16S rRNA, *Escherichia coli* O157:H7 16S rRNA, synthetic SARS-CoV-2 genes (Orf1ab-a, Orf1ab-b, S gene, E gene, N gene), and HIV virus RNA	∼10 copies per rxn (20 μL volume)	Lateral flow and fluorescence	50 minutes preamplification + 5–10 minutes cleavage reaction	149
dCas9	RT-RPA	Bunyavirus RNA, the causative agent of severe fever with thrombocytopenia syndrome (SFTS)	0.63 aM	Single microring resonator (SMR) biosensor	30 minutes	150
dCas9	LAMP	HIV-1	0.96 copies per mL	Bright field microscopy	70 minutes	152
dCas9	No	Epstein-Barr virus encoded RNA (EBER)	—	Fluorescence *in situ* hybridization (FISH)	20 minutes or less	157
dCas9	RCA	miRNAs (miRNA-195)	fM level	Colorimetric	∼4 hours	153

Table 3 (*continued*)

Type of enzyme	Preamplification	Target	LOD	Read out	Rxn time	Ref.
Cas9	No	SARS-CoV-2	3×10^8 copies of RNA	Gel electrophoresis, fluorescence	—	156
Cas9	No	Target RNA	Picomolar level	Denaturing polyacrylamide gel electrophoresis (PAGE)	—	158
Cas9	RCA	miRNA-21, miRNA-221	90 fM	Fluorescence	2 hours preamplification + 30–60 minutes cleavage reaction	154
Cas9	PCR	RFP transgene	—	Targeted sequencing	—	181
Cas9	Exponential amplification reaction (EXPAR)	*L. monocytogenes* hemolysin (hly) mRNA	0.82 aM	Fluorescence	—	151
Cas9	NASBA	Zika virus	—	Colorimetric	—	182
SpyCas9	RAA	Respiratory syncytial virus A	98 copies per μL	Fluorescence	2 hours 25 minutes	183
dCas9	RT-RPA	SARS-CoV-2	2.5 copies per μL	Lateral flow assay (LFA)	55 minutes	155

and cleaved by Cas9.[153] Cleavage of a TaqMan probe releases fluorescence, directly indicating the presence of the target. Similarly, the RCH system harnesses RCA to bring together split horseradish peroxidase (HRP) fragments mediated by dCas9 binding, resulting in a visible color change upon substrate reaction (Fig. 5c).[153,154]

Finally, aiming for the simplest and most portable format, the Vigilant platform was introduced. This system fuses dCas9 with the VirD2 relaxase to enable a lateral flow assay, where amplified biotinylated targets are captured by VirD2–dCas9 complexes tagged with FAM-labeled oligonucleotides. A standard lateral flow strip detects these complexes visually through streptavidin and anti-FAM antibodies, allowing rapid and accessible RNA diagnostics.[155]

Beyond preamplification-assisted methods, research has revealed that Cas9 can directly enable amplification-free RNA detection, offering simpler and faster diagnostic possibilities. A major breakthrough was LEOPARD, where reprogrammed tracrRNA allowed Cas9 to bind RNA targets and cleave fluorescent DNA reporters, enabling multiplexed RNA detection without amplification.[156] Expanding into imaging, Chen *et al.* introduced RCasFISH, using dCas9 combined with sgRNAs bearing MS2 aptamers. Upon binding to RNA inside fixed cells, fluorescent MS2 proteins visualize RNA targets without amplification, preserving spatial information with high specificity.[157]

Even more striking, Strutt *et al.* discovered that certain Cas9 homologs, such as *Staphylococcus aureus* Cas9 (SauCas9) and *Campylobacter jejuni* Cas9 (CjeCas9), can inherently recognize and cleave RNA without the need for a PAM or PAMmer, instead solely guided by sgRNA. This native RNA-targeting ability expands Cas9's potential for amplification-free RNA diagnostics and direct RNA manipulation in cells.[158]

4. RNA detection using CRISPR–Cas14 (Cas12f)

Cas14, also known as Cas12f, is the smallest effector in the type V CRISPR–Cas family and has recently gained attention for its strong *trans*-cleavage activity on single-stranded DNA (ssDNA). Although initially applied in DNA detection, Cas14a and Cas14a1 have been increasingly adapted for RNA diagnostics using strategies that convert RNA into DNA intermediates or activate the enzyme directly (Table 3).[75]

Several preamplification strategies have been employed to harness Cas14's potential in RNA detection. Among these, a dual amplification system developed by Shu *et al.* that integrates an entropy-driven circuit (EDC) with Cas14a showed significant performance enhancement. This one-pot setup continuously produces ssDNA activators that stimulate Cas14a's *trans*-cleavage, improving sensitivity by 100-fold over Cas14a alone (Fig. 5a).[159] In another approach, a rolling circle amplification (RCA)–Cas14 system enabled the detection of plant miRNAs without requiring reverse transcription. The ligation-triggered amplification and Cas14a activation provided single-nucleotide resolution and a detection limit as low as 1 pM, demonstrating applicability in plant molecular diagnostics.[160] In viral detection, Cas14a was paired with a RT-LAMP assay, using primers engineered with PAM sequences to enable

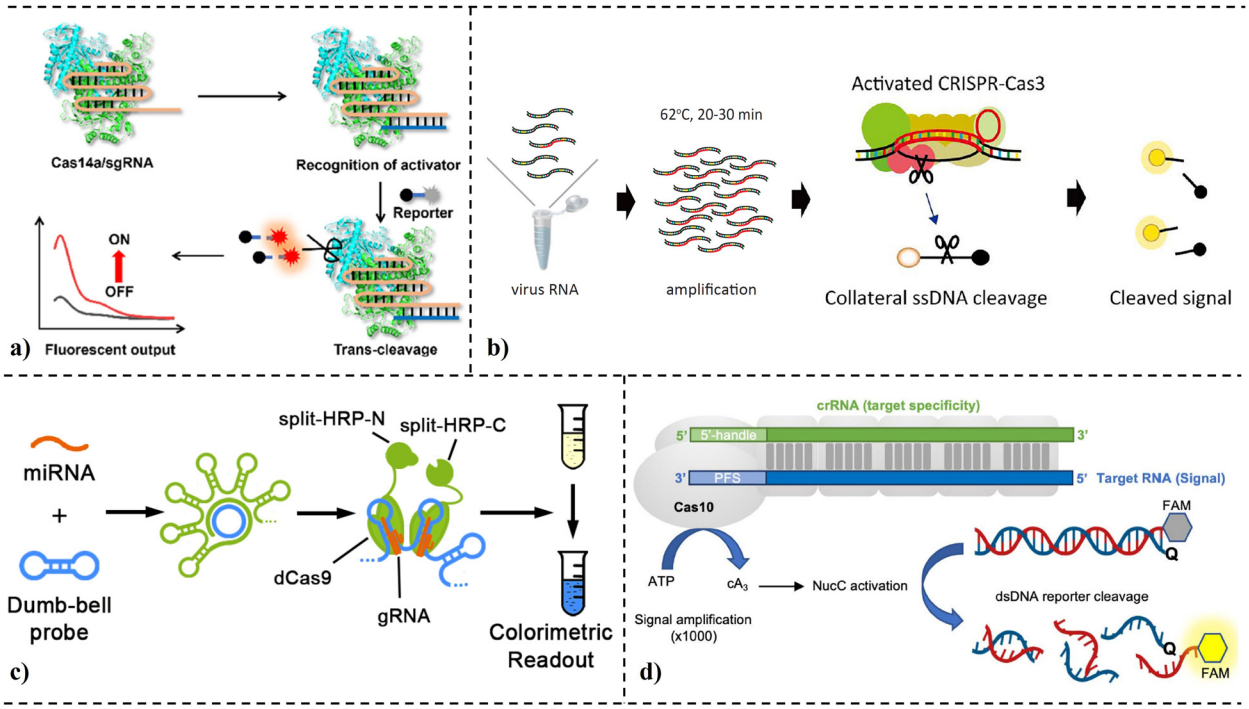

Fig. 5 (a) Scheme of the EDC–Cas14a system for miRNA detection, where the target generates multiple activators that trigger Cas14a/sgRNA collateral cleavage for signal amplification.[159] (b) Workflow of the CONAN RNA detection assay, including RNA extraction, RT-LAMP at 62 °C for 20–30 minutes, the CONAN reaction at 37 °C for 10 minutes, and lateral flow detection at room temperature for 2 minutes.[173] (c) Schematic of the RCH workflow for miRNA detection using RCA to amplify target signals into large DNA structures. CRISPR–dCas9 with split-HRP fusion enables secondary amplification by binding to RCA products.[153] (d) Outline of the type III CRISPR–Cas (Cmr)/NucC assay for RNA detection, where target RNA binding activates Cas10 to produce cA3 molecules. cA3 activates NucC, leading to degradation of a dsDNA reporter labeled with a fluorophore–quencher pair.[168] EDC: entropy-driven circuit; CONAN: CRISPR–Cas3-operated nucleic acid detection; RCH: rolling circle hybridization; RCA: rolling circle amplification; dCas9: catalytically dead CRISPR-associated protein 9; HRP: horseradish peroxidase.

Cas14a activation. This system achieved an impressive LOD of aM level, demonstrating exceptional sensitivity and compatibility with simplified magnetic bead-based RNA extraction.[161]

Additionally, Cas14a1 has been shown to function in asymmetric PCR-based assays for DNA diagnostics, with reported LODs down to the attomolar range. While primarily applied to DNA targets such as the SMN1 exon 7 deletion, these results support Cas14a1's potential for high-sensitivity nucleic acid detection. Most notably, Cas14a1 has also been shown to support amplification-free RNA detection.[162] A platform known as ATCas-RNA demonstrated that RNA can directly trigger Cas14a1's *trans*-cleavage activity without undergoing degradation. This system exhibited excellent specificity, including the ability to distinguish single-base mismatches, and achieved a remarkable LOD of 1 aM. By removing the need for reverse transcription or amplification, this method represents a major step forward in streamlining RNA diagnostics.[163]

In summary, Cas14a and Cas14a1 have proven to be flexible, powerful tools for RNA detection, operating effectively across diverse preamplification strategies, including EDC,[159] RCA,[160] SDA,[164] and RT-LAMP,[161] and excelling even in amplification-free[147] formats. Their compact size, high sensitivity, and programmability make them strong contenders for portable, rapid, and precise RNA diagnostics.

5. RNA detection using other CRISPR–Cas platforms

5.1. CRISPR–Cas10. While most CRISPR-based RNA diagnostic platforms have centered around type V (*e.g.*, Cas12) and type VI (*e.g.*, Cas13) systems, a growing number of studies have demonstrated the diagnostic potential of less conventional CRISPR–Cas effectors such as Cas10, Cas7–11, and Cas3 (Table 3). These systems offer unique mechanisms and modular components that expand the versatility of RNA detection approaches.

A notable example is Cas10, the signature effector of type III CRISPR–Cas systems, which has been successfully adapted for RNA detection using RT-LAMP-based preamplification.[165] In one study, the type III-A TtCsm complex from *Thermus thermophilus* was repurposed for RNA detection. Upon RNA target binding, the Cas10 subunit exhibited polymerase activity, producing cyclic oligoadenylates (cOAs), pyrophosphates, and protons. These by-products were detected using a combination of colorimetric dyes (*e.g.*, phenol red, malachite green), fluorometric reporters (calcein), and TtCsm6-activated fluorescent cleavage. Sensitivity was significantly enhanced by combining RT-LAMP with T7 transcription, reducing the detection limit from $\sim 10^8$ copies per reaction to 10^6 copies per mL in clinical samples, with results available in under an hour.[165]

A second study introduced SCOPE, a diagnostic platform based on the type III-B Cmr complex, which similarly used

RNA-activated Cas10 to generate cOAs. These activated a downstream CARF-domain RNase (TTHB144), which cleaved quenched RNA reporters to produce a fluorescent signal. In a two-step RT-LAMP–CRISPR workflow, SCOPE achieved a detection limit of 40 aM (~25 copies per μL) and demonstrated robust sensitivity even in a one-pot format (LOD: 800 aM). Reaction times varied between 35 minutes (two-step) and up to 180 minutes (one-pot), depending on the configuration.[166]

Beyond preamplification-based detection, recent studies have also explored amplification-free RNA diagnostics using Cas10. One approach utilized the VmeCmr complex from *Vibrio metoecus*, where RNA binding triggers Cas10 to generate cOAs, activating the nuclease NucC, which cleaves a DNA reporter (Fig. 5d).[167,168] Other amplification-free approaches have leveraged the direct RNA cleavage activity of Cas10-containing complexes. The *Staphylococcus epidermidis* Cas10–Csm complex demonstrated crRNA-guided ssRNA cleavage without amplification, while the LdCsm system from *Lactobacillus delbrueckii* achieved miRNA detection *via* Cas10-mediated collateral DNase activity, with a detection limit of 500 pM to 1 nM in buffer and ~2 nM in serum.[169] Additionally, the StCsm complex from *Sulfolobus tokodaii* was used in RNA editing applications, further supporting Cas10's intrinsic RNA-targeting capabilities.[170]

5.2. CRISPR–Cas7–11. Continuing with emerging systems, the type III-E CRISPR–Cas system, also known as craspase, introduces a distinct detection mechanism through Cas7–11, which functions not as a nuclease but as an RNA-guided protease. In this system, target ssRNA binding activates the Csx29 protease, which in turn cleaves a protein substrate, Csx30, providing a novel basis for RNA detection. Unlike traditional CRISPR-based detection systems that rely on nucleic acid cleavage, craspase utilizes engineered protein probes tagged with a fluorescent marker and His-tag. Upon cleavage, fluorescence is released into the supernatant and quantified, with signal increase indicating target RNA presence. This strategy allows for amplification-free detection down to 25 pM, and sensitivity improves to ~2 fM when combined with RT-RPA.[171]

While sensitivity remains slightly lower than platforms like DETECTR or SHERLOCK, the stability of protein probes and programmability of the protease system offer promising avenues for future clinical applications and assay expansion. In a separate approach, researchers developed a programmable RNA sensor named CASP, utilizing Cas7–11 (DiCas7–11) from *Desulfonema ishimotonii* as the RNA-binding component. Upon target RNA binding, Cas7–11 activates an associated protease (Csx29), triggering downstream gene expression *via* release of transcriptional effectors. A mutant version of Cas7–11 with deactivated ribonuclease activity showed 20-fold improved sensitivity. While highly sensitive to mid-to-high expression RNAs, the system faces challenges with low-abundance targets, suggesting further enhancement through signal amplification strategies.[172]

5.3. CRISPR–Cas3. Beyond class 2 systems, class 1 CRISPR–Cas3 effectors have also been repurposed for RNA detection, offering unique capabilities through their collateral ssDNA cleavage activity. Although primarily DNA-targeting, systems like the CRISPR–Cas3-operated nucleic acid detection (CONAN) assay adapted Cas3 for rapid and sensitive detection of RNA viruses. In CONAN, RNA is reverse-transcribed into cDNA, activating Cas3's *trans*-cleavage of nearby ssDNA reporters, enabling detection with single-copy sensitivity when paired with isothermal preamplification methods like RPA or LAMP[173] (Fig. 5b). Building on this, the discovery of a novel type I-A Cas3 variant from *Thermococcus siculi* (TsiCas3) introduced the hyperactive-verification establishment (HAVE) assay, achieving rapid (within 35 minutes) and accurate nucleic acid detection with strong resilience to harsh conditions.[174] Notably, TsiCas3 exhibited dual activation by both DNA and ssRNA, although direct ssRNA cleavage remains less efficient. Despite current sensitivity limitations compared to attomolar-level Cas12 or Cas13 systems, Cas3-based platforms like CONAN[173] and HAVE[174] highlighted the versatility and ruggedness of type I CRISPR enzymes for point-of-care RNA diagnostics, especially in resource-limited environments.

To better understand the characteristics and advantages of different CRISPR–Cas platforms for RNA diagnostics, we systematically compared the detection performance of major Cas enzyme families, such as Cas13, Cas12, Cas9, Cas14, Cas10, Cas7–11 (craspase), and Cas3, based on their molecular targets, collateral activities, preamplification requirements, sensitivity, specificity, assay time, thermal stability, and POC compatibility (Table 4). Each system exhibits distinct biochemical properties that influence its suitability for diagnostic applications. For instance, Cas13 systems are favored for direct RNA detection with high specificity and no need for reverse transcription,[68,72] while Cas12 enzymes, especially Cas12g, offer high thermal stability, better accessibility, and compatibility with visual or smartphone-based detection.[108] Emerging systems like Cas10 and Cas7–11 expand detection mechanisms to include signal relay and protease-based readouts, respectively.[168,171] Table 4 summarizes the key features of these systems, highlighting the trade-offs between sensitivity, speed, and ease of deployment in resource-limited settings.

6. Clinical applications

CRISPR–Cas systems have been extensively applied in the detection of disease-associated RNA targets, spanning both infectious diseases and cancer diagnostics. Various Cas enzymes have been harnessed to develop innovative RNA detection platforms. Among these, Cas13 stands out as the most commonly used due to its intrinsic RNA-targeting mechanism and potent collateral cleavage activity.[43,45] These technologies have enabled the detection of a wide range of clinically and biologically significant RNA molecules, from viral[175] genomes, bacterial transcripts,[179] to microRNAs[140] and messenger RNAs implicated in cancer. In the following sections, we explore the application of CRISPR-based diagnostics across different disease contexts, beginning with RNA-based pathogens, and then moving to cancer-related RNA biomarkers.

6.1. Infectious disease diagnostics (viral and bacterial RNA detection). RNA virus detection has been one of the most

Table 4 Comparative features of CRISPR–Cas platforms for RNA detection

Feature	Cas13	Cas12	Cas9	Cas14	Cas10	Cas7–11 (craspase)	Cas3
Target	RNA	Primarily DNA (*via* RT); Cas12g directly targets RNA	Primarily DNA; engineered for RNA	Primarily ssDNA; Cas14a1 adapted for RNA	RNA	RNA	Primarily DNA; adapted to RNA *via* RT
Collateral activity	*Trans*-cleaves RNA reporters	*trans*-Cleaves ssDNA reporters	Recently discovered: *trans*-cleaves both RNA and ssDNA reporters	*trans*-Cleaves ssDNA	Indirect *trans*-cleavage by triggering cyclic oligoadenylates (cOAs) synthesis and activation of downstream RNases	*trans*-Cleaves RNA reporters	*trans*-Cleaves ssDNA reporters
Preamplification requirement	Both preamplification-based and preamplification-free detection	Typically required; Cas12g is an exception	Often requires preamplification, but preamplification-free possible	Both preamplification and preamplification-free	Both preamplification and preamplification-free	Both preamplification and preamplification-free	Mostly preamplification
Sensitivity (w/o preamplification)	As low as 10 aM	As low as 10 fM	Picomolar range	As low as 1 aM	As low as 8 fM	25 pM	0.1–1 nM
Sensitivity (w/ preamplification)	~0.1 aM	~0.5 aM or single-copy detection	As low as 0.63 aM	As low as 0.6 aM	As low as 800 aM	~2 fM	Single-copy sensitivity
Turnover rate	1–740 s^{-1}	0.01–20 s^{-1}	—	<0.02 s^{-1}	0.01–0.5 s^{-1} for Csm6	—	0.01–10 s^{-1}
Assay speed	15–40 min	5–30 min	5–70 min	1–2 hours	10–180 min	~2 hours	15–42 min
Specificity (*e.g.*, SNP detection)	High	Very high	High	Very high	High	—	—
Thermal stability	Variable; generally, requires cold chain	High for engineered variants (*e.g.*, eBrCas12b at 67 °C)	—	—	Thermostable (TtCsm, TthB144)	—	Thermostable (TsiCas3)
POC compatibility	Excellent: portable, adaptable to fluorescent, lateral flow, electrochemical	Excellent: smartphone-based, paper-based, visual readouts	Smartphone, lateral flow, digital detection (*e.g.*, dCRISTOR)	Portable, magnetic bead-based, visual detection	Colorimetric/fluorescent, rugged for low-resource use	Fluorescent protein cleavage, protease-based sensing	Lateral flow, robust for field use
Limitations	Cold chain, reagent cost	Needs reverse transcription (except Cas12g), format complexity	Needs reverse transcription step, complex multiplexing, primarily DNA-targeting	Originally DNA-based, limited RNA usage without engineering	Lower sensitivity *vs.* Cas12/13, limited SNP selectivity	Lower sensitivity	Weak ssRNA cleavage, lower sensitivity

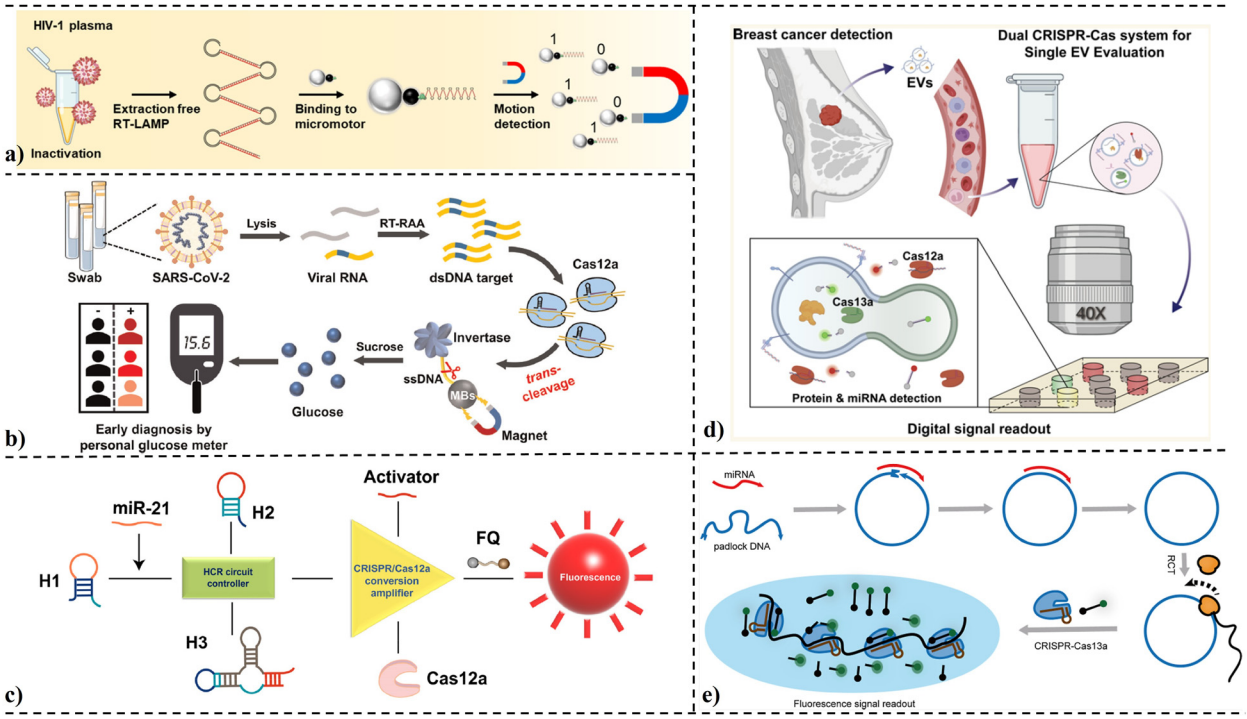

Fig. 6 (a) The control flow of HIV-1 detection using the dCRISTOR (dCas9) assay with CNN-MOT, combining inactivation, extraction-free RT-LAMP, micromotor binding to LAMP amplicons, and motion-based detection.[152] (b) Working mechanism of a CRISPR–Cas12a-based biosensor that allows quantitative RNA detection through a portable personal glucose meter readout.[184] (c) Workflow of HCR combined with Cas12a for miR-21 detection.[86] (d) Overview of the digital dual CRISPR–Cas-powered single EV evaluation (ddSEE) system design.[190] (e) miRNA detection by miRoll-Cas for prostate cancer diagnosis.[191] dCRISPR: digital clustered regularly interspaced short palindromic repeats; CNN-MOT: convolutional neural network classification-based multiobject tracking algorithm; HCR: hybridization chain reaction; miRoll-Cas: microRNA rolling circle amplification-Cas system.

prominent applications of CRISPR diagnostics, with Cas13 used extensively due to its inherent RNA-targeting capability. Among the RNA viruses, SARS-CoV-2 has been the most studied, prompting the development of numerous Cas13-based assays.[51] Innovative amplification-free approaches such as hydrogel-based capillary flow sensors have enabled visual and quantitative detection of viral RNA directly from clinical samples, with detection limits reaching the attomolar range.[61] To further enhance sensitivity, various signal amplification strategies have been introduced, including catalytic hairpin assembly (CHA)[50,51] and hybridization chain reaction (HCR), allowing for enzyme-free yet ultrasensitive detection. The flexibility of crRNA design has also enabled discrimination between viral strains by exploiting single-nucleotide differences. These strategies are now being adapted to other RNA viruses such as Influenza, Dengue, Ebola, Zika, and HCV, demonstrating the broad potential of CRISPR-based diagnostics for viral detection.[41]

6.1.1. SARS-CoV-2. CRISPR-based detection systems have been widely applied for the detection of SARS-CoV-2 RNA, offering advantages such as rapid detection, high sensitivity, and compatibility with point-of-care testing. Multiple Cas enzymes, including Cas12aCCC,[128] Cas12b,[106] Cas13a,[39] type III Cas systems (Cas10,[166] Cas7–11[171]), Cas3, have been explored across different diagnostic formats.

In the realm of Cas12 enzymes, researchers leveraged both Cas12a and Cas12b to build diverse diagnostic platforms for SARS-CoV-2 (Fig. 6b).[184] One amplification-free method used Cas12a with magnetic bead-assisted separation and manganese-enhanced fluorescence signaling, enabling detection within 45 minutes with a LOD of 2.2 pM.[95] Another Cas12a-based system integrated toehold-mediated strand displacement reactions (TSDR), converting RNA into DNA activators that triggered Cas12a's transcleavage activity, achieving ultrasensitive electrochemical detection down to 40 aM.[138] In a parallel effort, Ning *et al.* demonstrated an RT-RPA-Cas12a-based assay capable of ultrasensitive and quantitative detection of SARS-CoV-2 directly from saliva samples, bypassing the need for conventional nasal swabs. Remarkably, this work was also among the first to integrate CRISPR diagnostics with smartphone readout, enabling portable and accessible testing. The combination of high sensitivity, non-invasive sampling, and smartphone compatibility positioned this platform as a promising tool for point-of-care COVID-19 diagnostics.[79] Separately, the iSCAN-V2 platform integrated RT-RPA with Cas12b, showing enhanced performance over Cas12a and achieving reliable detection at 40 copies per μL using a low-cost fluorescence readout device.[106]

Cas13a added another dimension with the SATCAS platform, which integrated reverse transcription, amplification, and detection in a one-pot setup. It achieved single-copy

detection (~aM range) within 40 minutes, proving effective in clinical validation.[31] Meanwhile, type III CRISPR enzymes introduced alternative mechanisms, Cas10 in the SCOPE platform produced cyclic oligoadenylates (cOAs) upon RNA recognition, activating CARF-domain nucleases for signal generation.[166] A type III-B complex (VmeCmr) utilized cA3 signaling to trigger NucC nuclease activity, allowing direct SARS-CoV-2 RNA detection at 2 fM without preamplification.[171]

Additionally, Cas3 has been adapted into the CONAN assay, which utilizes EcoCas3's collateral ssDNA cleavage activity for SARS-CoV-2 RNA detection, offering a rapid and low-cost diagnostic alternative.[173] In addition to Cas3-based systems, Cas9 has also been adapted for diagnostic use through the Vigilant platform. The vigilant platform repurposes dCas9 fused with VirD2 to detect SARS-CoV-2 RNA after RT-RPA amplification. By binding the target sequence and linking to a FAM-labelled probe, it enables visual detection on a lateral flow strip. Vigilant offers a low detection limit (2.5 copies per μL), high sensitivity (96.4%), and perfect specificity (100%), making it a simple and cost-effective tool for point-of-care diagnostics.[155]

6.1.2. Hepatitis-associated RNA viruses (HCV and HDV). CRISPR technology has shown remarkable adaptability in detecting hepatitis C virus (HCV) RNA, leveraging various Cas enzymes to enhance sensitivity and clinical utility. One of the standout methods is the SPLENDID platform, which integrates RT-LAMP with a thermostable engineered Cas12b (eBrCas12b) in a single-pot format. This setup simplifies the detection process while maintaining high accuracy, achieving 97.5% specificity and 90% overall accuracy in clinical serum samples.[103] In contrast, the SAHARA system employed Cas12a to detect HCV RNA without requiring reverse transcription. By exploiting Cas12a's unique ability to recognize RNA at the PAM-distal end of the crRNA, when anchored by a short PAM-containing DNA fragment, this method enabled direct detection. Pooling multiple crRNAs targeting different regions of the HCV genome improved performance, reaching a detection limit of 132 pM, although RNA secondary structure still posed a challenge.[98]

Cas13a has also been explored for HCV diagnostics, especially for amplification-free strategies. Screening 13 distinct crRNAs revealed that pooling them significantly enhanced Cas13a's *trans*-cleavage efficiency, improving assay sensitivity for RNA detection. The same approach was extended to hepatitis D virus (HDV), where CRISPR–Cas13a was combined with RT-PCR or RT-RAA for detection. These methods offered strong performance and were visualized using lateral flow strips, demonstrating the system's potential in both laboratory and POC settings.[185]

6.1.3. Human immunodeficiency virus (HIV). CRISPR-based technologies have been effectively adapted for the detection of HIV RNA, demonstrating strong potential for sensitive, specific, and POC diagnostics.[186] One notable approach employs a CRISPR-mediated cascade reaction (CRISPR-MCR) biosensor integrating RT-RPA amplification with Cas12a detection. In this system, Cas12a is activated upon recognition of amplified HIV RNA, leading to cleavage of ssDNA-invertase conjugates immobilized on magnetic beads. This platform achieved a detection sensitivity of 200 copies of HIV RNA per test and was successfully validated using clinical plasma samples.[112]

Another approach combines RT-RAA amplification with Cas13a-mediated detection for HIV-1 RNA. This system uses a degenerate base-binding Cas13a–crRNA complex. Results are visualized using a lateral flow strip, offering a portable, rapid, and user-friendly format. The assay demonstrated a limit of detection of 1 copy per μL, with 91.81% sensitivity and 100% specificity in clinical evaluations, detecting viral loads as low as 112 copies per mL.[187]

Additionally, the dCRISTOR (Fig. 6a) assay uses dCas9-functionalized magnetic micromotors to bind amplified HIV-1 RNA and convert target presence into a binary digital signal. The system combines extraction-free LAMP, magnetic motion tracking, and deep learning for simple, label-free detection. It achieved 100% sensitivity and specificity in plasma samples, with a detection limit of 0.96 copies per μL, making it a low-cost and effective tool for point-of-care HIV diagnostics.[152]

6.1.4. Ebola virus. CRISPR-based detection systems have shown considerable promise for the detection of Ebola virus RNA, offering speed, specificity, and potential for point-of-care diagnostics. Two major approaches using different Cas enzymes have been explored:

A key innovation is the Cas-Roller assay, which employs Cas13a from *Leptotrichia wadei* (LwaCas13a) for direct RNA detection without amplification. Upon recognition of Ebola RNA, the Cas13a–crRNA complex is activated and cleaves a specially designed RNA-modified DNA hairpin probe attached to gold nanoparticles. The cleavage releases a single-stranded DNA "leg" that initiates a DNA nanomachine *via* catalytic hairpin assembly (CHA), leading to an amplified fluorescent signal. This system achieved a limit of detection as low as 291 aM (~175 copies per μL) and completed the detection process in about 40 minutes at 37 °C.[69]

In a separate approach, Cas12a was incorporated into a microfluidic paper-based analytical device (mPAD), where it was combined with reverse transcription-recombinase polymerase amplification (RT-RPA) to detect synthetic Ebola genomic RNA. This method achieved a limit of detection of 11 aM, underscoring the ultra-sensitive capabilities of CRISPR-based detection when paired with isothermal amplification techniques.[110]

6.1.5. RNA respiratory viruses. CRISPR-based diagnostics have demonstrated strong potential for the sensitive and specific detection of RNA respiratory viruses. Both Cas12a and Cas13a enzymes have been applied in various formats to target these pathogens.

A notable development is the LOC-CRISPR microfluidic system, which employs Cas12a to detect multiple respiratory viruses, including SARS-CoV-2 variants (BA.1, BA.2, BA.5), H1N1, H3N2, influenza B virus (IVB), and human respiratory

syncytial virus (HRSV). This chip-based platform integrates nucleic acid extraction, isothermal amplification (RPA), and Cas12a-mediated cleavage in a sealed, contamination-free format. Clinical validation showed 97.8% sensitivity and 100% specificity, with detection possible for viral RNA concentrations as low as 100 copies per mL within 60 minutes.[111] Another Cas12a-based method, designed for rabies virus RNA, combines target binding-induced isothermal amplification with Cas12a's *trans*-cleavage activity. This electrochemiluminescence biosensor achieved a detection limit of 2.8 pM, offering high sensitivity and specificity without relying on complex instrumentation.[135]

6.1.6. Flaviviruses and similar arboviruses. CRISPR diagnostics has shown great promise in addressing arboviruses such as Dengue virus (DENV) and Zika virus (ZIKV), both members of the Flavivirus genus. Two distinct approaches underscore the versatility of CRISPR technology for these viruses, one focused on ultrasensitive detection, the other on therapeutic inhibition.

For DENV detection, an electrochemical biosensor was developed using the CRISPR–Cas12a system. This method exploits the *trans*-cleavage activity of Cas12a, activated upon recognition of a DNA analog of DENV-4 RNA, to cleave a methylene blue (MB)-linked ssDNA probe immobilized on gold nanoparticles. Cleavage of the probe results in a measurable decrease in electrochemical signal, enabling sensitive detection. This system achieved a detection limit of 100 fM for DENV-4 RNA without any RNA amplification and demonstrated high specificity by discriminating against other DENV serotypes and unrelated viral RNA sequences, including ZIKV.[142]

In contrast, the ZIKV study employed a CRISPR–Cas13b system not for detection but for targeted inhibition of viral replication in mammalian cells. crRNAs designed against conserved regions of the ZIKV genome successfully guided Cas13b to cleave viral RNA, reducing infection levels. A fluorescent reporter system (mCherry fused to the ZIKV capsid) was used to quantify viral load, offering a potential foundation for diagnostic development.[188] To improve strain-level detection of Zika virus, researchers developed NASBACC, a low-cost CRISPR/Cas9-based diagnostic module integrated with NASBA amplification. By exploiting Cas9's sequence-specific cleavage, NASBACC can distinguish between closely related Zika strains based on single-nucleotide differences. This adds a crucial layer of specificity to paper-based diagnostics, enabling accurate strain identification while remaining portable and suitable for low-resource settings.[182]

6.1.7. Bacterial RNA detection. CRISPR-based diagnostic systems have also been effectively adapted for the detection of bacterial RNA. Various Cas enzymes, especially Cas13a,[60] Cas12a,[141] and more recently Cas14a1,[162] have been utilized in these platforms.

One notable strategy uses Cas13a in an amplification-free electrochemiluminescence (ECL) biosensor for detecting *Escherichia coli* O157:H7 RNA. This system exploits Cas13a's transcleavage activity to cleave self-enhanced ECL probes upon target recognition. The result is signal amplification without the need for nucleic acid amplification or co-reactants. This method demonstrated rapid detection (~20 minutes), a wide linear detection range, and strong specificity, including successful application to clinical urine and blood samples.[60]

Another approach incorporates Cas12a in a method called T7/G4-CRISPR, which enables sensitive detection of bacterial RNA such as 16S rRNA. This assay converts a single RNA target into many DNA activators *via* a toehold-mediated strand displacement and T7 exonuclease-assisted recycling circuit. The DNA activators trigger Cas12a's *trans*-cleavage, preventing assembly of a split G-quadruplex (G4) reporter, leading to a measurable fluorescence decrease. The platform showed improved sensitivity over direct detection, was able to distinguish single-nucleotide variants, and was validated against clinical urine samples, avoiding complex thermal cycling.[141]

More recently, Cas14a1 has been shown to directly respond to RNA, leading to the development of the ATCas-RNA platform. This system uses RNA to activate Cas14a1's *trans* ssDNA cleavage activity, achieving high specificity and ultralow detection limits (attomolar range). It was successfully applied to detect bacterial RNA in contaminated milk samples, extending Cas14a1's utility beyond its original DNA-targeting scope.[162]

6.2. Cancer biomarker detection (miRNA-based CRISPR diagnostics). MicroRNAs (miRNAs) have emerged as crucial biomarkers in cancer diagnosis and prognosis due to their differential expression in various types of tumors. These small, non-coding RNAs play vital roles in regulating gene expression and are often found to be upregulated or downregulated in cancerous tissues compared to healthy ones. Detecting specific miRNAs associated with cancer has thus become a valuable strategy for early diagnosis, monitoring progression, and evaluating treatment response.[89,129,140] To enable effective analysis from clinical biofluids, microfluidic systems offer high-throughput, label-free separation of low-abundance miRNAs and CTCs, supporting upstream preparation for molecular diagnostics.[189]

CRISPR-based systems, particularly those involving Cas12a and Cas13a, have been extensively adapted to detect cancer-related miRNAs with high sensitivity and specificity. By integrating these enzymes with amplification strategies or signal transduction mechanisms, researchers have developed robust platforms capable of detecting miRNAs in clinical samples such as blood, serum, urine, and tissue lysates.[44,145]

In the following subsections, we explore how different CRISPR–Cas-based systems have been applied to detect miRNA biomarkers associated with specific types of cancer, including lung, breast, colorectal, prostate, and glioblastoma. Each subsection highlights the key miRNAs linked to these cancers and summarizes CRISPR strategies developed for their detection.

6.2.1. Lung cancer biomarker. The application of CRISPR-based detection systems for detecting lung cancer biomarkers has opened exciting new possibilities for early, non-invasive cancer diagnosis. In particular, miRNAs, small RNA molecules known for their regulatory roles, have gained attention as powerful biomarkers for non-small-cell lung carcinoma

(NSCLC). Their aberrant expression in cancerous tissues compared to healthy controls makes them attractive and accessible targets for molecular diagnostics. Among the various Cas enzymes, Cas12a,[85] Cas13a,[33] Cas12j,[107] cas9,[154] and LdCsm (a Cas10-related system)[169] have been effectively adapted for lung cancer miRNA analysis, offering rapid, sensitive, and highly specific detection strategies.

Among these, miR-21 stands out as the most commonly targeted marker, consistently overexpressed in lung cancer samples. It has been detected using a range of CRISPR–Cas systems from serum, plasma, and cell lysates with attomolar sensitivity.[86] Similarly, miR-155, another key biomarker, has been identified using Cas12a-driven electrochemical sensors[84] and the LdCsm system,[169] showing excellent specificity suitable for point-of-care applications.

Broader panels including miR-17, miR-92a, and EGFR mRNA[33] have also been investigated using Cas13a-based electrochemical biosensors. These platforms can measure multiple targets on a single chip, distinguishing early-stage NSCLC from healthy samples. Cas12j, a more recently explored enzyme, was used to sensitively detect miR-21 and miR-92a in plasma, delivering results comparable to RT-qPCR standards.[107]

Further innovations extended to diagnostic validation. For example, miR-195 was used in an RCA-CRISPR-split-HRP (RCH) assay to confirm the specificity of NSCLC-targeted miRNA detection. The platform correctly showed no differential miR-195 expression between NSCLC patients and healthy individuals, reinforcing its accuracy.[33]

In another study, the Cas9-based RACE system was used to detect miR-221, miR-21, and miR-222 simultaneously. By coupling RCA with Cas9-mediated cleavage, the system generated fluorescent signals correlating to miRNA abundance in extracellular vesicles from lung cancer samples. Its results matched RT-qPCR, supporting its potential for clinical use.[154]

6.2.2. Breast cancer biomarker. CRISPR-based technologies, particularly those employing Cas12a and Cas14a, have been extensively adapted for the sensitive and specific detection of breast cancer-associated miRNAs.[85] Key targets include miR-10b and miR-21, both known for their significant roles in breast cancer progression and metastasis (Fig. 6d).[86,96,159,190]

The detection of miR-21, one of the most studied biomarkers, has led to the development of several CRISPR/Cas12a-based approaches. These included systems combining split T7 polymerase transcription with Cas12a for fluorescence-based detection,[134] electrochemical sensing platforms that simultaneously detected miR-21 and miR-155,[85] and Au-nanobeacon biosensors achieving direct, attomolar-level sensitivity without the need for RNA amplification.[96] Additional strategies, such as entropy-driven catalysis cycles, hybridization chain reaction (HCR) controllers, and hyperbranched rolling circle amplification (HRCA) coupled with Cas12a, further boosted detection sensitivity, reaching femtomolar limits (Fig. 6c).[86] In another approach, platforms like SCas12a, employing split crRNA designs, enabled amplification-free and multiplexed detection of mature miRNAs, maintaining strong agreement with traditional RT-qPCR results.[102]

On the other hand, for miR-10b, another microRNA associated with breast cancer, an entropy-driven circuit (EDC) integrated with Cas14a enabled dual amplification, dramatically enhancing sensitivity and allowing detection even in complex samples like serum and cell lysates. This method capitalized on continuous ssDNA activator production to robustly trigger Cas14a's *trans*-cleavage activity.[159]

6.2.3. Colorectal cancer biomarker. In addition to miRNA detection in lung and breast cancers, the techniques and strategies developed with CRISPR-based detection systems also offer strong potential for adaptation to colorectal cancer diagnostics. The powerful RNA-targeting capabilities of Cas enzymes like Cas13a,[33] Cas12a,[99] and Cas12j[107] have led to the creation of highly sensitive, specific, and innovative miRNA detection platforms.

Among these technologies, the COMET system stands out, using Cas13a in combination with a catalytic hairpin DNA circuit (CHDC) to achieve two-stage signal amplification. This system successfully detected a panel of RNAs associated with non-small-cell lung carcinoma (NSCLC), including miR-17, miR-155, miR-19b, and miR-210, demonstrating its capacity to distinguish cancer patients from healthy individuals through analysis of serum samples. The high sensitivity of the COMET platform, capable of attomolar detection, highlights its adaptability for other cancers like colorectal cancer.[33]

In another approach, researchers utilized an asymmetric CRISPR assay based on Cas12a, leveraging competitive crRNA binding to enhance cascade signal amplification without the need for reverse transcription. This system demonstrated successful quantitative detection of miR-19a in plasma samples from bladder cancer patients, achieving excellent correlation with RT-qPCR results.[99]

Additionally, the EXP-J assay, employing Cas12j, further advanced miRNA detection by coupling exponential amplification reaction (EXPAR) with Cas12j's *trans*-cleavage activity. Applied to lung cancer biomarkers, the method effectively detected miR-21 and miR-92a in plasma samples, yielding results that closely matched traditional RT-qPCR data. The success of EXP-J in clinical samples suggests strong potential for its application in detecting colorectal cancer-associated miRNAs.[107]

6.2.4. Prostate cancer biomarker. In recent years, CRISPR/Cas12a systems have been at the forefront of developing highly sensitive tools for detecting miRNAs associated with prostate cancer. Although the reviewed studies were not solely focused on prostate cancer, they reveal powerful strategies for miRNA analysis that directly target miR-141 (Fig. 6e),[127,191] and miR-21,[86] two miRNAs widely recognized as important biomarkers in prostate cancer progression and diagnosis.

The detection strategies center around the *trans*-cleavage activity of Cas12a. Upon recognizing a target-specific crRNA and a corresponding activator DNA sequence, Cas12a is activated and begins cleaving surrounding single-stranded DNA (ssDNA) reporters like fluorescence-based systems, and

electrochemiluminescence (ECL)-based biosensors, generating strong and measurable signals. Signal amplification played a crucial role in boosting sensitivity.[132] Strategies like the 3D DNA walker helped convert a single miRNA-141 molecule into multiple DNA activators, while hybridization chain reaction (HCR) circuits amplified the pre-crRNA needed for Cas12a activation. These smart designs allowed researchers to achieve extremely low detection limits, reaching the femtomolar and even attomolar range.[127]

While the primary applications were broader than just prostate cancer, the strong focus on miR-141 and miR-21 detection clearly signals the high potential of CRISPR-based diagnostics for prostate cancer screening. With their rapid detection times, high sensitivity, and ability to adapt to portable formats, these systems pave the way for future POC applications and early cancer diagnostics.

6.2.5. Glioblastoma biomarker. CRISPR technologies have opened new horizons in the sensitive detection of miRNAs related to aggressive cancers like glioblastoma.[137] Initially, CRISPR/Cas12a systems faced limitations in direct RNA detection, as they required a complete crRNA structure to activate their powerful *trans*-cleavage activity. To overcome this, scientists engineered the mini crRNA-mediated CRISPR/Cas12a system (MCM-CRISPR/Cas12a). This innovation enabled partial crRNA structures to function effectively without compromising their *trans*-cleavage potential, allowing direct detection of non-coding RNAs like miRNAs. Using the MCM-CRISPR/Cas12a platform, researchers achieved impressive sensitivity levels, down to 10 pM for miRNA-21, a miRNA strongly linked to glioblastoma. To push the detection limits even further, they combined the MCM system with amplification strategies such as hybridization chain reaction (HCR) and catalytic hairpin assembly (CHA). This powerful combination drove detection sensitivity into the femtomolar range, achieving 2.5 fM for miRNA-21, 8.98 fM for miRNA-128-3p, and 81.6 fM for lncRNA PACER.[87]

In a complementary study, researchers designed a novel sensor that integrated upconverted nanoparticles (UCNPs) with the CRISPR/Cas12a system, leveraging a dual enzymatic amplification strategy using exonuclease III (Exo III) and phi29 DNA polymerase. Upon near-infrared light activation, a hairpin probe on the UCNPs bound to miRNA-21, triggering Exo III-mediated recycling and subsequent rolling circle amplification (RCA) *via* phi29 polymerase. The resulting amplified RNA sequences activated Cas12a, which cleaved a fluorescent reporter to produce a strong, detectable signal. This dual amplification platform achieved a remarkable limit of detection of 6.01 fM for miRNA-21 and demonstrated excellent performance in real biological samples, including serum and cell lysates from cancer cell lines like MCF-7 and HeLa.[137] Moreover, both studies confirmed that these CRISPR-based approaches offer excellent specificity, showing minimal cross-reactivity with non-target miRNAs, a critical feature for clinical application.

In essence, the combination of innovative crRNA designs, advanced signal amplification strategies, and the precise activity of Cas12a is pushing CRISPR technology toward becoming a transformative tool for cancer biomarker detection, offering the promise of earlier and more accurate cancer diagnostics.

7. Agricultural applications

Recently, a variety of biosensors employing diverse sensing mechanisms have been developed for plant health and gas monitoring, aiming to advance sustainable agriculture and environmental management.[192–195] CRISPR-based biosensors have recently emerged as powerful tools for detecting RNA biomarkers associated with plant diseases, offering new capabilities for monitoring plant health and improving crop yield outcomes.[196] Isothermal reaction conditions, rapid response times, high sensitivity and specificity, and simplified workflows make CRISPR diagnostic platforms one of the most appealing diagnostic methods for agricultural applications, especially well-suited for in-field tracking of plant pathogens and insect infestations, enhancing disease surveillance and precision agriculture applications.[197] In order to detect RNA-based analytes for tracking plant and insect infestations in agricultural applications, CRISPR–Cas13 and CRISPR–Cas12 assays have been mostly applied to directly and indirectly detect RNAs, respectively.

Recent studies have demonstrated the utility of CRISPR-based platforms for detecting various plant-related RNA targets with high sensitivity and future prospects for crop field compatibility. For instance, tomato spotted wilt virus (TSWV) in tomato and thrips was detected using an indirect Cas13a-based assay following RPA amplification, achieving a detection limit of 2.26×10^2 copies per μL with a sensor response in 20 minutes.[198] The glyphosate resistance gene transcript in soybean was detected indirectly using LwaCas13a *via* the SHERLOCK platform, providing a LOD of 2 aM.[199] Banana ripeness profiling was demonstrated through direct detection of 1.839 pM.[160] Tomato brown rugose fruit virus (ToBRFV), a major threat to solanaceous crops, was detected indirectly *via* LbCas12a in conjunction with RT-LAMP, offering detection sensitivity comparable to RT-qPCR and enabling visual detection in field settings.[200]

Mixed infections involving tobacco mosaic virus (TMV), tobacco etch virus (TEV), and potato virus X (PVX) were diagnosed using both Cas12a (indirect, *via* RT) and Cas13a/d (direct), with Cas13 also enabling viral load quantification and compatibility with lateral flow strips.[201] Rice black-streaked dwarf virus (RBSDV) was detected indirectly using RfxCas13d, integrated with isothermal amplification for field deployment, achieving detection of only a few RNA copies.[49] Maize chlorotic mottle virus (MCMV), a serious quarantine pathogen in maize production, was detected using Cas12a paired with RT-RAA, allowing visual fluorescence-based detection at dilutions as low as 10^{-5} from 2000 ng of total RNA.[202] These recent findings highlight the significant potential of CRISPR diagnostic platforms for detecting RNA targets in agricultural applications.[196,197]

8. Environmental applications

RNA detection using CRISPR/Cas platforms could also be useful for various environmental applications, such as tracking waterborne pathogens, including viral and bacterial RNAs (*e.g.*, *E. coli*,

Listeria, SARS-CoV-2), that may exist in drinking and surface water. It would also be valuable for monitoring pathogens or antibiotic resistance genes in wastewater systems. In addition, CRISPR-based RNA detection could help identify RNA signatures from pathogens or transgenic organisms to mitigate their presence in farms, which could impact both agricultural productivity and environmental health. This approach could also serve as a rapid detector of zoonotic viruses or parasites in natural ecosystems, while aiding in the detection of invasive or endangered species. Importantly, it could be used to detect RNA-based contaminants in food and soil, supporting improved biosafety and ecological monitoring.[203]

A recent study demonstrated the applicability of the Cas13a platform to detect RNA targets from the 16S rRNA gene of *Cyprinus carpio* and *Oryzias latipes*. *C. carpio* is an invasive species that disrupts aquatic ecosystems, while *O. latipes* is a native model species widely used in ecological research. In addition, the study showed that Cas13a could detect environmental RNA (eRNA) from filtered water samples, highlighting its potential for monitoring invasive species to mitigate biodiversity threats, tracking endangered species in aquatic systems, and supporting habitat conservation. This platform enables on-site detection of live organisms in ecosystems and facilitates real-time biodiversity surveillance in dynamic environmental conditions. The Cas13a assay achieved a LOD as low as 1 copy per μL for *C. carpio* RNA and 1000 copy per μL for *O. latipes* RNA.[46]

In addition, future perspectives have proposed the integration of CRISPR platforms for RNA detection into marine biomonitoring systems, aiming to enable rapid, sensitive, and on-site detection of environmental RNA targets such as those from harmful algal blooms (HABs), marine pathogens, and invasive species, with the support of AI-driven CRISPR RNA design for enhanced precision and field deployment.[204]

9. Challenges and future directions

While CRISPR/Cas-based technologies offer great versatility for RNA detection and have rapidly advanced over the past few years, several challenges still hinder their optimal efficiency in targeting RNA molecules.[16,19,205] We categorize the current challenges into four key aspects: (1) biological, (2) readout performance and sample preparation, (3) scalability and cost-effectiveness, and (4) real-world clinical considerations. We also propose future prospects to advance CRISPR-based biosensors for RNA detection by addressing each of these identified challenges.

From the biological aspect, factors such as variability in efficacy among different Cas enzymes, off-target (non-target) detection issues, indirect or direct RNA detection mechanism, the frequent need for preamplification steps to achieve ultra-high sensitivity, the use of low-yield or non-specific guide RNAs for various diseases, and the biological stability of reagents all critically influence the efficiency of CRISPR/Cas platforms.[16,19,205] Minimizing off-target effects and designing unique, high-yield, and efficient guide RNAs (gRNAs) through the use of machine learning and bioinformatics platforms could significantly reduce non-specific detection and enhance robust performance across diverse sequence contexts—both of which remain key areas of ongoing research.[206,207] Also, synergistic innovation in both crRNA and DNA activator design is recommended to enhance the biological aspects of CRISPR/Cas platforms for RNA detection, considering the following key aspects. For crRNA design, future advancements are expected to focus on structurally dynamic architectures such as split,[102] caged,[208] or switchable[209] crRNAs, which allow conditional activation of the CRISPR–Cas system in response to specific RNA targets. Additionally, for *in vivo* diagnostic platforms, incorporating chemically modified nucleotides is expected to improve crRNA stability against nuclease degradation.[210] On the DNA activator side, to reduce background signals, utilizing refined toehold-mediated strand displacement systems is recommended.[211,212] Also, integrating aptamers[213] into activators can expand detection capabilities beyond nucleic acids. Finally, to facilitate the construction of more intelligent diagnostic platforms capable of multi-input processing and decision-making, the development of nucleic acid-based logic circuits (*e.g.*, AND, OR gates) is recommended.[214] Together, these innovative strategies provide promising opportunities to significantly increase the sensitivity, specificity, and flexibility of next-generation CRISPR diagnostics.

From the result readout aspect, the lack of digitized and portable platforms restricts the broader deployment of CRISPR diagnostics. Many existing systems still rely on conventional laboratory instruments such as plate readers or fluorescence microscopes, limiting their use in POC or field settings.[215] The development of integrated, portable, and user-friendly readout systems, such as smartphone-based readers, is critical to unlocking the full potential of CRISPR technologies for decentralized testing.[216–218] From the sample preparation aspect, the complexity of upstream sample handling remains a major bottleneck. Many biological samples require nucleic acid extraction and purification to remove inhibitors that can interfere with amplification or Cas activity.[12,219] Therefore, innovations such as rapid lysis methods compatible with CRISPR reactions, microfluidic sample prep systems,[220] and integrated "sample-to-answer"[221] platforms are paramount to truly enable field-deployable CRISPR diagnostics.

From the scalability and cost-effectiveness aspect, several factors inhibit the mass adoption of CRISPR-based diagnostics. These include the relatively high costs and availability of reagents (Cas enzymes, guide RNAs, reporters), the complexity of device fabrication for POC use, and the need for regulatory approval processes such as those required by the FDA.[12] Also the need for cold chain storage of Cas proteins and RNA components significantly restricts the deployment of CRISPR-based diagnostics in remote or resource-limited settings. Addressing this issue requires the development of thermostable Cas variants[222] that can remain functional at ambient temperatures.

Finally, from the real clinical application aspect,[223] challenges such as multiplexed detection where multiple targets need to be detected simultaneously remain.[224] While the programmability of CRISPR offers exciting potential for multiplexing,

practical issues such as guide RNA cross-reactivity, optimization of multiple Cas–gRNA reactions in a single assay, and clear signal differentiation still need to be systematically addressed. Additionally, while delivery of CRISPR-based detection systems into cells is less critical for *ex vivo* diagnostics, it becomes a major challenge for any potential *in vivo* applications, demanding further advancements in safe and efficient delivery methods.[225]

Conclusion

CRISPR–Cas systems have rapidly emerged as a transformative force in RNA diagnostics, offering unmatched programmability, specificity, and adaptability for a diverse array of biomedical applications. This review has outlined both the fundamental mechanisms and technological innovations underlying RNA detection using a broad spectrum of Cas effectors, including Cas12, Cas13, Cas14, Cas9, Cas10, Cas3, and the recently characterized Cas7–11. Through preamplification-based and amplification-free approaches, these systems now support rapid, sensitive, and highly specific detection across multiple contexts such as infectious diseases (*e.g.*, SARS-CoV-2, HIV, HCV, ZIKV) and cancer-related biomarkers (*e.g.*, miRNAs in NSCLC).

Particularly, Cas13's innate RNA-targeting capability has driven major advances in amplification-free detection, while Cas12a and Cas12b have demonstrated powerful one-pot isothermal amplification strategies suited for POC deployment. Cas9, traditionally a DNA-targeting enzyme, has been ingeniously re-engineered for RNA diagnostics, expanding its utility across imaging, amplification, and digital quantification platforms. Meanwhile, class 1 systems like Cas3 and Cas10 contribute unique signal amplification routes and ruggedness for low-resource applications. Emerging platforms, including Cas7–11-based protease sensors and Cas14-driven ultrasensitive assays, further push the boundaries of detection sensitivity and modular design.

Despite tremendous progress, ongoing challenges such as improving sensitivity in amplification-free systems, multiplexing capacity, and field-deployable integration remain focal points for future development. Nonetheless, the convergence of CRISPR technology with advanced biosensing, microfluidics, and AI-driven signal analysis signals a promising future for decentralized, rapid, and precise RNA diagnostics. As these tools continue to mature, their integration into clinical workflows has the potential to revolutionize early disease detection, therapeutic monitoring, and pandemic preparedness on a global scale.

Author contributions

MB conducted the literature review, prepared the figures, and drafted the manuscript. SJ assisted in summarizing the findings, contributed to drafting the manuscript, and prepared schematic figures. AS assisted in interpreting the findings and contributed to drafting the manuscript. Q. W. supervised the project, provided critical revisions, and contributed to the final manuscript. All authors read and approved the final version.

Conflicts of interest

The authors declare that they have no conflict of interest.

Data availability

No primary research results, software or code have been included and no new data were generated or analysed as part of this review.

Acknowledgements

The authors sincerely thank funding support from the National Science Foundation (Award # 1944167) for this work.

Notes and references

1 F. Crick, *Nature*, 1970, **227**, 561–563.
2 Imaging of endogenous RNA in live cells using sequence-activated fluorescent RNA probes|Nucleic Acids Research|Oxford Academic, **https://academic.oup.com/nar/article/53/2/gkae1209/7919505?login=false**, (accessed April 30, 2025).
3 Sensors for surveillance of RNA viruses: a One Health perspective – The Lancet Microbe, **https://www.thelancet.com/journals/lanmic/article/PIIS2666-5247(24)00297-0/fulltext**, (accessed April 30, 2025).
4 X. Xi, T. Li, Y. Huang, J. Sun, Y. Zhu, Y. Yang and Z. J. Lu, *Noncoding RNAs*, 2017, **3**, 9.
5 Y. Li and S. Sun, *EMBO J.*, 2025, **44**, 613–638.
6 T. A. Omran, I. L. Madsø, P. C. Sæther, V. Bemanian and H. S. Tunsjø, *Sci. Rep.*, 2024, **14**, 27468.
7 Comparison of RT-qPCR and RT-dPCR Platforms for the Trace Detection of SARS-CoV-2 RNA in Wastewater|ACS ES&T Water, **https://pubs.acs.org/doi/10.1021/acsestwater.1c00387**, (accessed April 30, 2025).
8 Impact of RNA Isolation Protocols on RNA Detection by Northern Blotting|SpringerLink, **https://link.springer.com/protocol/10.1007/978-1-4939-2547-6_4**, (accessed April 30, 2025).
9 A. Yaqoob, N. K. Verma, R. M. Aziz and M. A. Shah, *J. Cancer Res. Clin. Oncol.*, 2024, **150**, 455.
10 J. Lai and J. Jedrych, *J. Cutaneous Pathol.*, 2025, **52**, 266–268.
11 MicroRNA detection by microarray|Analytical and Bioanalytical Chemistry, **https://link.springer.com/article/10.1007/s00216-008-2570-2**, (accessed April 30, 2025).
12 A. Ghouneimy, A. Mahas, T. Marsic, R. Aman and M. Mahfouz, *ACS Synth. Biol.*, 2022, **12**, 1–16.
13 History of CRISPR–Cas from Encounter with a Mysterious Repeated Sequence to Genome Editing Technology|Journal of Bacteriology, **https://journals.asm.org/doi/full/10.1128/jb.00580-17**, (accessed April 30, 2025).
14 P. Horvath and R. Barrangou, *Science*, 2010, **327**, 167–170.
15 RNA targeting with CRISPR–Cas13|Nature, **https://www.nature.com/articles/nature24049**, (accessed April 30, 2025).
16 M. Burmistrz, K. Krakowski and A. Krawczyk-Balska, *Int. J. Mol. Sci.*, 2020, **21**, 1122.
17 Z. Weng, Z. You, J. Yang, N. Mohammad, M. Lin, Q. Wei, X. Gao and Y. Zhang, *Angew. Chem., Int. Ed.*, 2023, **62**, e202214987.
18 N. Mohammad, S. S. Katkam and Q. Wei, *CRISPR J.*, 2022, **5**, 500–516.
19 RNA-targeting CRISPR–Cas systems|Nature Reviews Microbiology, **https://www.nature.com/articles/s41579-022-00793-y**, (accessed April 30, 2025).
20 T. Zhu, W. Jiang, Y. Wu, R. Fang, F. Deng and D. Yang, *Talanta*, 2025, 128223.

21 C. Zhu, C. Liu, X. Qiu, S. Xie, W. Li, L. Zhu and L. Zhu, *Biotechnol. Bioeng.*, 2020, **117**, 2279–2294.
22 F. X. Liu, J. Q. Cui, Z. Wu and S. Yao, *Lab Chip*, 2023, **23**, 1467–1492.
23 M. M. Kaminski, O. O. Abudayyeh, J. S. Gootenberg, F. Zhang and J. J. Collins, *Nat. Biomed. Eng.*, 2021, **5**, 643–656.
24 R. Aman, A. Mahas and M. Mahfouz, *ACS Synth. Biol.*, 2020, **9**, 1226–1233.
25 H. Li, Y. Xie, F. Chen, H. Bai, L. Xiu, X. Zhou, X. Guo, Q. Hu and K. Yin, *Chem. Soc. Rev.*, 2023, **52**, 361–382.
26 A. Bonini, N. Poma, F. Vivaldi, A. Kirchhain, P. Salvo, D. Bottai, A. Tavanti and F. Di Francesco, *J. Pharm. Biomed. Anal.*, 2021, **192**, 113645.
27 S. Chen, R. Wang, C. Lei and Z. Nie, *Chem. Res. Chin. Univ.*, 2020, **36**, 157–163.
28 W. Feng, H. Zhang and X. C. Le, *Anal. Chem.*, 2023, **95**, 206–217.
29 L. B. Harrington, D. Burstein, J. S. Chen, D. Paez-Espino, E. Ma, I. P. Witte, J. C. Cofsky, N. C. Kyrpides, J. F. Banfield and J. A. Doudna, *Science*, 2018, **362**, 839–842.
30 J. S. Gootenberg, O. O. Abudayyeh, J. W. Lee, P. Essletzbichler, A. J. Dy, J. Joung, V. Verdine, N. Donghia, N. M. Daringer and C. A. Freije, *Science*, 2017, **356**, 438–442.
31 T. Wang, L. Bai, G. Wang, J. Han, L. Wu, X. Chen, H. Zhang, J. Feng, Y. Wang and R. Wang, *Biosens. Bioelectron.*, 2024, **263**, 116636.
32 X. Wang, X. Deng, Y. Zhang, W. Dong, Q. Rao, Q. Huang, F. Tang, R. Shen, H. Xu and Z. Jin, *Biosens. Bioelectron.*, 2024, **257**, 116268.
33 Y. Sheng, T. Zhang, S. Zhang, M. Johnston, X. Zheng, Y. Shan, T. Liu, Z. Huang, F. Qian and Z. Xie, *Biosens. Bioelectron.*, 2021, **178**, 113027.
34 W. Liu, H. Li, J. Tao, L. Wang, J. Hu and C. Zhang, *Nano Today*, 2024, **59**, 102529.
35 D. Zhao, J. Tang, Q. Tan, X. Xie, X. Zhao and D. Xing, *Talanta*, 2023, **260**, 124582.
36 J. Zhang, C. Song, Y. Zhu, H. Gan, X. Fang, Q. Peng, J. Xiong, C. Dong, C. Han and L. Wang, *Biosens. Bioelectron.*, 2023, **219**, 114836.
37 Y. Li, Q. Wang and Y. Wang, *J. Anal. Sci. Technol.*, 2024, **15**, 21.
38 T. Hu, Y. Yu, Y. Lin and C. Chen, *Anal. Chem.*, 2023, **95**, 18587–18594.
39 D. Wang, X. Wang, F. Ye, J. Zou, J. Qu and X. Jiang, *ACS Nano*, 2023, **17**, 7250–7256.
40 K. Wang, H. Yin, S. Li, Y. Wan, M. Xiao, X. Yuan, Z. Huang, Y. Gao, J. Zhou and K. Guo, *Biosens. Bioelectron.*, 2025, **267**, 116825.
41 A. M. Molina Vargas, S. Sinha, R. Osborn, P. R. Arantes, A. Patel, S. Dewhurst, D. J. Hardy, A. Cameron, G. Palermo and M. R. O'Connell, *Nucleic Acids Res.*, 2024, **52**, 921–939.
42 C. Zhang, P. Zhang, H. Ren, P. Jia, J. Ji, L. Cao, P. Yang, Y. Li, J. Liu, Z. Li, M. You, X. Duan, J. Hu and F. Xu, *Chem. Eng. J.*, 2022, **446**, 136864.
43 Y. Tian, Z. Fan, X. Zhang, L. Xu, Y. Cao, Z. Pan, Y. Mo, Y. Gao, S. Zheng, J. Huang, H. Zou, Z. Duan, H. Li and F. Ren, *Emerging Microbes Infect.*, 2023, **12**, 2276337.
44 P. Song, P. Zhang, K. Qin, F. Su, K. Gao, X. Liu and Z. Li, *Talanta*, 2022, **246**, 123521.
45 M. Patchsung, K. Jantarug, A. Pattama, K. Aphicho, S. Suraritdechachai, P. Meesawat, K. Sappakhaw, N. Leelahakorn, T. Ruenkam, T. Wongsatit, N. Athipanyasilp, B. Eiamthong, B. Lakkanasirorat, T. Phoodokmai, N. Niljianskul, D. Pakotiprapha, S. Chanarat, A. Homchan, R. Tinikul, P. Kamutira, K. Phiwkaow, S. Soithongcharoen, C. Kantiwiriyawanitch, V. Pongsupasa, D. Trisrivirat, J. Jaroensuk, T. Wongnate, S. Maenpuen, P. Chaiyen, S. Kamnerdnakta, J. Swangsri, S. Chuthapisith, Y. Sirivatanauksorn, C. Chaimayo, R. Sutthent, W. Kantakamalakul, J. Joung, A. Ladha, X. Jin, J. S. Gootenberg, O. O. Abudayyeh, F. Zhang, N. Horthongkham and C. Uttamapinant, *Nat. Biomed. Eng.*, 2020, **4**, 1140–1149.
46 J. Yang, S. Matsushita, F. Xia, S. Yoshizawa and W. Iwasaki, *Methods Ecol. Evol.*, 2024, **15**, 1408–1421.
47 I. L. Calderón, M. J. Barros, N. Fernández-Navarro and L. G. Acuña, *Microorganisms*, 2024, **12**, 283.
48 Y. Wang, Y. Hou, X. Liu, N. Lin, Y. Dong, F. Liu, W. Xia, Y. Zhao, W. Xing and J. Chen, *World J. Microbiol. Biotechnol.*, 2024, **40**, 51.
49 L. Li, C. Duan, J. Weng, X. Qi, C. Liu, X. Li, J. Zhu and C. Xie, *Sci. China: Life Sci.*, 2022, **65**, 1456–1465.
50 Y. Yang, W. Yi, F. Gong, Z. Tan, Y. Yang, X. Shan, C. Xie, X. Ji, Z. Zheng and Z. He, *Anal. Chem.*, 2023, **95**, 1343–1349.
51 X. Gao, Y. Yin, J. Xie, S. Gong and X. Li, *Sens. Actuators, B*, 2025, **422**, 136706.
52 Z. Zhang, J. Li, C. Chen, Y. Tong, D. Liu, C. Li, H. Lu, L. Huang, W. Feng and X. Sun, *Anal. Chim. Acta*, 2024, **1300**, 342409.
53 J. Zhong, Z. Xu, J. Peng, L. Guan, J. Li, Z. Zhou, Y. Zhang, J. Zhang, S. Liu and Y. Yang, *Talanta*, 2025, **291**, 127852.
54 L. Guan, J. Peng, T. Liu, S. Huang, Y. Yang, X. Wang and X. Hao, *Anal. Chem.*, 2023, **95**, 17708–17715.
55 N. Yan, Z. Hu and L. Zhang, *Appl. Biochem. Biotechnol.*, 2024, **196**, 7896–7907.
56 J. Wei, Z. Song, J. Cui, Y. Gong, Q. Tang, K. Zhang, X. Song and X. Liao, *J. Hazard. Mater.*, 2023, **452**, 131268.
57 Y. Dou, Y. He, H. Zhang, M. Yang, Q. Liu, W. Ma, X. Fu and Y. Chen, *Anal. Methods*, 2024, **16**, 6810–6818.
58 Y. Zhan, X. Gao, S. Li, Y. Si, Y. Li, X. Han, W. Sun, Z. Li and F. Ye, *Front. Cell. Infect. Microbiol.*, 2022, **12**, 904485.
59 S. Li, F. Wang, L. Hao, P. Zhang, G. Song, Y. Zhang, C. Wang, Z. Wang and Q. Wu, *Int. J. Biol. Macromol.*, 2024, **283**, 137594.
60 X. Liu, S. Zhou, R. Sun, K. Ye, Y. Lu, A. He, Y. Yang, J. Lin, J. Hu and C. Zhang, *Sens. Actuators, B*, 2025, **426**, 137048.
61 H. Wang, H. Wang, H. Pian, F. Su, F. Tang, D. Chen, J. Chen, Y. Wen, X. C. Le and Z. Li, *Anal. Chem.*, 2024, **96**, 12022–12029.
62 T. Li, D. Chen, X. He, Z. Li, Z. Xu, R. Li, B. Zheng, R. Hu, J. Zhu and Y. Li, *Chem. Commun.*, 2024, **60**, 3166–3169.
63 Q. He, Q. Chen, L. Lian, J. Qu, X. Yuan, C. Wang, L. Xu, J. Wei, S. Zeng and D. Yu, *Microchim. Acta*, 2024, **191**, 466.
64 Y. Zhang, P. Miao, J. Wang, Y. Sun, J. Zhang, B. Wang and M. Yan, *Sensors*, 2024, **24**, 6138.
65 S. Mantena, P. P. Pillai, B. A. Petros, N. L. Welch, C. Myhrvold, P. C. Sabeti and H. C. Metsky, *Nat. Biotechnol.*, 2024, 1–8.
66 L. Cheng, F. Yang, Y. Zhao, Z. Liu, X. Yao and J. Zhang, *Biosens. Bioelectron.*, 2023, **222**, 114982.
67 J. Dong, X. Wu, Q. Hu, C. Sun, J. Li, P. Song, Y. Su and L. Zhou, *Biosens. Bioelectron.*, 2023, **241**, 115673.
68 L. Kashefi-Kheyrabadi, H. V. Nguyen, A. Go and M.-H. Lee, *Bioelectrochemistry*, 2023, **150**, 108364.
69 X.-M. Hang, P.-F. Liu, S. Tian, H.-Y. Wang, K.-R. Zhao and L. Wang, *Biosens. Bioelectron.*, 2022, **211**, 114393.
70 Y. Xue, X. Luo, W. Xu, K. Wang, M. Wu, L. Chen, G. Yang, K. Ma, M. Yao, Q. Zhou, Q. Lv, X. Li, J. Zhou and J. Wang, *Anal. Chem.*, 2023, **95**, 966–975.
71 H. Zeng, P. Zhang, X. Jiang, C. Duan, Y. Yu, Q. Wu and X. Yang, *Anal. Chim. Acta*, 2022, **1217**, 340009.
72 I. Azmi, M. I. Faizan, R. Kumar, S. Raj Yadav, N. Chaudhary, D. Kumar Singh, R. Butola, A. Ganotra, G. Datt Joshi and G. Deep Jhingan, *Front. Cell. Infect. Microbiol.*, 2021, **11**, 632646.
73 L. Liu, Z. Wang, Y. Wang, J. Luan, J. J. Morrissey, R. R. Naik and S. Singamaneni, *Adv. Healthcare Mater.*, 2021, **10**, 2100956.
74 K. Guk, S. Yi, H. Kim, Y. Bae, D. Yong, S. Kim, K.-S. Lee, E.-K. Lim, T. Kang and J. Jung, *Biosens. Bioelectron.*, 2023, **219**, 114819.
75 J. E. van Dongen, J. T. W. Berendsen, R. D. M. Steenbergen, R. M. F. Wolthuis, J. C. T. Eijkel and L. I. Segerink, *Biosens. Bioelectron.*, 2020, **166**, 112445.
76 Z. Li, H. Zhang, R. Xiao, R. Han and L. Chang, *Nat. Chem. Biol.*, 2021, **17**, 387–393.
77 S.-Y. Li, Q.-X. Cheng, J.-M. Wang, X.-Y. Li, Z.-L. Zhang, S. Gao, R.-B. Cao, G.-P. Zhao and J. Wang, *Cell Discovery*, 2018, **4**, 20.
78 B. Ning, B. M. Youngquist, D. D. Li, C. J. Lyon, A. Zelazny, N. J. Maness, D. Tian and T. Y. Hu, *Cells Rep. Methods*, 2022, **2**(2), 100173.
79 B. Ning, T. Yu, S. Zhang, Z. Huang, D. Tian, Z. Lin, A. Niu, N. Golden, K. Hensley and B. Threeton, *Sci. Adv.*, 2021, **7**, eabe3703.
80 B. Pang, J. Xu, Y. Liu, H. Peng, W. Feng, Y. Cao, J. Wu, H. Xiao, K. Pabbaraju and G. Tipples, *Anal. Chem.*, 2020, **92**, 16204–16212.
81 R. Wang, C. Qian, Y. Pang, M. Li, Y. Yang, H. Ma, M. Zhao, F. Qian, H. Yu, Z. Liu, T. Ni, Y. Zheng and Y. Wang, *Biosens. Bioelectron.*, 2021, **172**, 112766.
82 P. Ma, Q. Meng, B. Sun, B. Zhao, L. Dang, M. Zhong, S. Liu, H. Xu, H. Mei, J. Liu, T. Chi, G. Yang, M. Liu, X. Huang and X. Wang, *Adv. Sci.*, 2020, **7**, 2001300.
83 Z. Zhu, Y. Guo, C. Wang, Z. Yang, R. Li, Z. Zeng, H. Li, D. Zhang and L. Yang, *Biosens. Bioelectron.*, 2023, **228**, 115179.
84 X. Li, J. Dong, L. Deng, D. Huo, M. Yang and C. Hou, *Talanta*, 2025, **286**, 127413.

85 J. Dong, C. Hou, L. Deng, T. Gu, S. Zhu, J. Hou and D. Huo, *Anal. Chem.*, 2025, **97**, 1028–1036.
86 K. Long, G. Cao, Y. Qiu, N. Yang, J. Chen, M. Yang, C. Hou and D. Huo, *Talanta*, 2024, **266**, 125130.
87 X. Chen, C. Huang, J. Zhang, Q. Hu, D. Wang, Q. You, Y. Guo, H. Chen, J. Xu and M. Hu, *Talanta*, 2024, **268**, 125350.
88 X. Zhang, H. Li, W. Zhao, J. Xu, S. Wang and R. Yu, *Microchim. Acta*, 2023, **190**, 458.
89 Z. Guo, X. Tan, H. Yuan, L. Zhang, J. Wu, Z. Yang, K. Qu and Y. Wan, *Talanta*, 2023, **252**, 123837.
90 L. Zhang, Z. Zhang, R. Liu, S. Wang, L. Li, P. Zhao, Y. Wang, S. Ge and J. Yu, *Sens. Actuators, B*, 2023, **394**, 134334.
91 Y. Xu, B. Chen, M. He, G. Yuan and B. Hu, *Anal. Chem.*, 2025, **97**, 811–817.
92 N. Aggarwal, Y. Liang, J. L. Foo, H. Ling, I. Y. Hwang and M. W. Chang, *Biosens. Bioelectron.*, 2023, **222**, 115002.
93 F. S. Silva, E. Erdogmus, A. Shokr, H. Kandula, P. Thirumalaraju, M. K. Kanakasabapathy, J. M. Hardie, L. G. Pacheco, J. Z. Li and D. R. Kuritzkes, *Adv. Mater. Technol.*, 2021, **6**, 2100602.
94 B. Fang, Z. Jia, C. Liu, K. Tu, M. Zhang and L. Zhang, *Talanta*, 2022, **249**, 123657.
95 D. Li, Y. Yao, W. Cheng, F. Yin, M. He and Y. Xiang, *Sens. Actuators, B*, 2025, **426**, 137154.
96 T. Luo, J. Li, Y. He, H. Liu, Z. Deng, X. Long, Q. Wan, J. Ding, Z. Gong, Y. Yang and S. Zhong, *Anal. Chem.*, 2022, **94**, 6566–6573.
97 J. Zhang, W. Yin, Q. Jiang, W. Mao, W. Deng, S. Jin, X. Wang, R. He, J. Qiao and Y. Liu, *Commun. Biol.*, 2025, **8**, 366.
98 S. R. Rananaware, E. K. Vesco, G. M. Shoemaker, S. S. Anekar, L. S. W. Sandoval, K. S. Meister, N. C. Macaluso, L. T. Nguyen and P. K. Jain, *Nat. Commun.*, 2023, **14**, 5409.
99 J. Moon and C. Liu, *Nat. Commun.*, 2023, **14**, 7504.
100 X. Fei, C. Lei, W. Ren and C. Liu, *Nucleic Acids Res.*, 2025, **53**, gkaf002.
101 Z. Hu, S. Ling, J. Duan, Z. Yu, Y. Che, S. Wang, S. Zhang, X. Zhang and Z. Li, *Nucleic Acids Res.*, 2025, **53**, gkaf017.
102 Y. Chen, X. Wang, J. Zhang, Q. Jiang, B. Qiao, B. He, W. Yin, J. Qiao and Y. Liu, *Nat. Commun.*, 2024, **15**, 8342.
103 L. T. Nguyen, S. R. Rananaware, L. G. Yang, N. C. Macaluso, J. E. Ocana-Ortiz, K. S. Meister, B. L. M. Pizzano, L. S. W. Sandoval, R. C. Hautamaki, Z. R. Fang, S. M. Joseph, G. M. Shoemaker, D. R. Carman, L. Chang, N. R. Rakestraw, J. F. Zachary, S. Guerra, A. Perez and P. K. Jain, *Cell Rep. Med.*, 2023, **4**(5), 101037.
104 J. Joung, A. Ladha, M. Saito, M. Segel, R. Bruneau, M.-L. W. Huang, N.-G. Kim, X. Yu, J. Li, B. D. Walker, A. L. Greninger, K. R. Jerome, J. S. Gootenberg, O. O. Abudayyeh and F. Zhang, *medRxiv*, 2020, preprint, DOI: 10.1101/2020.05.04.20091231.
105 X. Wu, C. Chan, S. L. Springs, Y. H. Lee, T. K. Lu and H. Yu, *Anal. Chim. Acta*, 2022, **1196**, 339494.
106 R. Aman, T. Marsic, G. Sivakrishna Rao, A. Mahas, Z. Ali, M. Alsanea, A. Al-Qahtani, F. Alhamlan and M. Mahfouz, *Front. Bioeng. Biotechnol.*, 2022, **9**, 800104.
107 J. Kang, H. Kim, Y. Lee, H. Lee, Y. Park, H. Jang, J. Kim, M. Lee, B. Jeong and J. Byun, *Adv. Sci.*, 2024, **11**, 2402580.
108 M. Liu, Z. Li, J. Chen, J. Lin, Q. Lu, Y. Ye, H. Zhang, B. Zhang and S. Ouyang, *PLoS Genet.*, 2023, **19**, e1010930.
109 A. Garcia-Venzor, B. Rueda-Zarazua, E. Marquez-Garcia, V. Maldonado, A. Moncada-Morales, H. Olivera, I. Lopez, J. Zuñiga and J. Melendez-Zajgla, *Front. Med.*, 2021, **8**, 627679.
110 M. A. English, L. R. Soenksen, R. V. Gayet, H. de Puig, N. M. Angenent-Mari, A. S. Mao, P. Q. Nguyen and J. J. Collins, *Science*, 2019, **365**, 780–785.
111 J. Shen, Z. Chen, R. Xie, J. Li, C. Liu, Y. He, X. Ma, H. Yang and Z. Xie, *Biosens. Bioelectron.*, 2023, **237**, 115523.
112 Z. Li, N. Uno, X. Ding, L. Avery, D. Banach and C. Liu, *ACS Nano*, 2023, **17**, 3966–3975.
113 R. Aman, A. Mahas, T. Marsic, N. Hassan and M. M. Mahfouz, *Front. Microbiol.*, 2020, **11**, 610872.
114 T. Wang, H. Zeng, J. Kang, L. Lei, J. Liu, Y. Zheng, W. Qian and C. Fan, *Pol. J. Microbiol.*, 2024, **73**, 253.
115 J. Jiao, K. Kong, J. Han, S. Song, T. Bai, C. Song, M. Wang, Z. Yan, H. Zhang and R. Zhang, *Plant Biotechnol. J.*, 2021, **19**, 394–405.
116 R. Zhao, Y. Xiao, Y. Tang, B. Lu and B. Li, *ACS Sens.*, 2024, **9**, 4803–4810.
117 H. Liu, M.-M. Lv, X. Li, M. Su, Y.-G. Nie and Z.-M. Ying, *Biosens. Bioelectron.*, 2025, **272**, 117106.
118 H. Yu, M. Feng, C. Liu, F. Wang, S. Pan, G. Sui, W. Jing and X. Cheng, *Int. J. Biol. Macromol.*, 2025, **290**, 138996.
119 Y. Chen, N. Zong, F. Ye, Y. Mei, J. Qu and X. Jiang, *Anal. Chem.*, 2022, **94**, 9603–9609.
120 R. Liu, Y. Hu, Y. He, T. Lan and J. Zhang, *Chem. Sci.*, 2021, **12**, 9022–9030.
121 M. Qing, S. L. Chen, Z. Sun, Y. Fan, H. Q. Luo and N. B. Li, *Anal. Chem.*, 2021, **93**, 7499–7507.
122 Y. Zhou, S. Xie, B. Liu, C. Wang, Y. Huang, X. Zhang and S. Zhang, *Anal. Chem.*, 2023, **95**, 3332–3339.
123 S. Zhou, M. Liu, L. Deng, Y. Qiu, T. Gu, J. Chen, M. Yang, D. Huo and C. Hou, *Sens. Actuators, B*, 2024, **408**, 135490.
124 W. Jiang, Z. Chen, J. Lu, X. Ren and Y. Ma, *Talanta*, 2023, **251**, 123784.
125 H. Chen, Z. Zhuang, Y. Chen, C. Qiu, Y. Qin, C. Tan, Y. Tan and Y. Jiang, *Anal. Chim. Acta*, 2023, **1246**, 340896.
126 L. Luo, F. Dong, D. Li, X. Li, X. Li, Y. Fan, C. Qi, J. Luo, L. Li and B. Shen, *ACS Sens.*, 2024, **9**, 1438–1446.
127 Q. Wang, Y. Liu, J. Yan, Y. Liu, C. Gao, S. Ge and J. Yu, *Anal. Chem.*, 2021, **93**, 13373–13381.
128 X.-M. Hang, H.-Y. Wang, P.-F. Liu, K.-R. Zhao and L. Wang, *Biosens. Bioelectron.*, 2022, **216**, 114683.
129 P. Chen, L. Wang, P. Qin, B.-C. Yin and B.-C. Ye, *Biosens. Bioelectron.*, 2022, **207**, 114152.
130 X. Wang, F. Wang, J. Wang, Y. Liu, C. Gao, S. Ge and J. Yu, *Sens. Actuators, B*, 2022, **370**, 132480.
131 X. Wang, H. Chen, M. Sun, B. Chen, H. Xu, Y. Fan, H. Zhou and J. Liu, *Sens. Actuators, B*, 2025, **425**, 137016.
132 Q. Wang, Z. Zhang, L. Zhang, Y. Liu, L. Xie, S. Ge and J. Yu, *ACS Appl. Mater. Interfaces*, 2022, **14**, 32960–32969.
133 M. Karlikow, E. Amalfitano, X. Yang, J. Doucet, A. Chapman, P. S. Mousavi, P. Homme, P. Sutyrina, W. Chan and S. Lemak, *Nat. Commun.*, 2023, **14**, 1505.
134 D. Li, W. Cheng, F. Yin, Y. Yao, Z. Wang and Y. Xiang, *Chem. Commun.*, 2025, **61**, 4555–4558.
135 S. Liu, C. Wang, Z. Wang, K. Xiang, Y. Zhang, G.-C. Fan, L. Zhao, H. Han and W. Wang, *Biosens. Bioelectron.*, 2022, **204**, 114078.
136 L. Zhang, Z. Zhang, Y. Zheng, S. Wang, L. Ruifang, L. Zhu, C. Li, L. Xie, S. Ge and J. Wu, *Sens. Actuators, B*, 2025, **426**, 137140.
137 W. Zhao, X. Zhang, R. Tian, H. Li, S. Zhong and R. Yu, *Sens. Actuators, B*, 2023, **393**, 134238.
138 K. Shi, Z. Yi, Y. Han, J. Chen, Y. Hu, Y. Cheng, S. Liu, W. Wang and J. Song, *Anal. Biochem.*, 2023, **664**, 115046.
139 S. Feng, H. Chen, Z. Hu, T. Wu and Z. Liu, *ACS Appl. Mater. Interfaces*, 2023, **15**, 28933–28940.
140 Y. Kang, J. Zhang, L. Zhao and H. Yan, *Biotechniques*, 2023, **74**, 172–178.
141 D. Zhang, B. Tian, Y. Ling, L. Ye, M. Xiao, K. Yuan, X. Zhang, G. Zheng, X. Li and J. Zheng, *Anal. Chem.*, 2024, **96**, 10451–10458.
142 Y. Lee, J. Choi, H.-K. Han, S. Park, S. Y. Park, C. Park, C. Baek, T. Lee and J. Min, *Sens. Actuators, B*, 2021, **326**, 128677.
143 B. Tian, Y. Wang, W. Tang, J. Chen, J. Zhang, S. Xue, S. Zheng, G. Cheng, B. Gu and M. Chen, *Talanta*, 2024, **266**, 124995.
144 S. Zhao, Q. Zhang, R. Luo, J. Sun, C. Zhu, D. Zhou and X. Gong, *Chem. Sci.*, 2024, **15**, 18347–18354.
145 L. Li, S. Li, N. Wu, J. Wu, G. Wang, G. Zhao and J. Wang, *ACS Synth. Biol.*, 2019, **8**, 2228–2237.
146 S. Li, J. Huang, L. Ren, W. Jiang, M. Wang, L. Zhuang, Q. Zheng, R. Yang, Y. Zeng and L. D. W. Luu, *Talanta*, 2021, **233**, 122591.
147 C. Jiao, N. L. Peeck, J. Yu, M. Ghaem Maghami, S. Kono, D. Collias, S. L. Martinez Diaz, R. Larose and C. L. Beisel, *Nat. Commun.*, 2024, **15**, 5909.
148 W. X. Yan, P. Hunnewell, L. E. Alfonse, J. M. Carte, E. Keston-Smith, S. Sothiselvam, A. J. Garrity, S. Chong, K. S. Makarova and E. V. Koonin, *Science*, 2019, **363**, 88–91.
149 T. Wang, Y. Wang, P. Chen, B.-C. Yin and B.-C. Ye, *Anal. Chem.*, 2022, **94**, 12461–12471.
150 B. Koo, D. Kim, J. Kweon, C. E. Jin, S.-H. Kim, Y. Kim and Y. Shin, *Sens. Actuators, B*, 2018, **273**, 316–321.
151 M. Huang, X. Zhou, H. Wang and D. Xing, *Anal. Chem.*, 2018, **90**, 2193–2200.
152 Y. Song, H. Park, P. Thirumalaraju, N. Kovilakath, J. M. Hardie, A. Bigdeli, Y. Bai, S. Chang, J. Yoo and M. K. Kanakasabapathy, *ACS Nano*, 2025, **19**, 8646–8660.

153 X.-Y. Qiu, L.-Y. Zhu, C.-S. Zhu, J.-X. Ma, T. Hou, X.-M. Wu, S.-S. Xie, L. Min, D.-A. Tan and D.-Y. Zhang, *ACS Synth. Biol.*, 2018, **7**, 807–813.
154 R. Wang, X. Zhao, X. Chen, X. Qiu, G. Qing, H. Zhang, L. Zhang, X. Hu, Z. He and D. Zhong, *Anal. Chem.*, 2019, **92**, 2176–2185.
155 T. Marsic, Z. Ali, M. Tehseen, A. Mahas, S. Hamdan and M. Mahfouz, *Nano Lett.*, 2021, **21**, 3596–3603.
156 C. Jiao, S. Sharma, G. Dugar, N. L. Peeck, T. Bischler, F. Wimmer, Y. Yu, L. Barquist, C. Schoen and O. Kurzai, *Science*, 2021, **372**, 941–948.
157 K. Chen, M. Wang, R. Zhang and J. Li, *Anal. Biochem.*, 2021, **625**, 114211.
158 S. C. Strutt, R. M. Torrez, E. Kaya, O. A. Negrete and J. A. Doudna, *eLife*, 2018, **7**, e32724.
159 X. Wang, P. Lv, C. Zhao, N. Yin, T. Fei, Y. Shu and J. Wang, *Sens. Actuators, B*, 2023, **397**, 134666.
160 H. Yang, J. Chen, S. Yang, T. Zhang, X. Xia, K. Zhang, S. Deng, G. He, H. Gao and Q. He, *Anal. Chem.*, 2021, **93**, 12602–12608.
161 X. Yang, L. Lu, Y. Luo, Q. Wang, J. Wang, Y. Ren, Y. Wu, M. Negahdary, K. E. Yunusov and S. A. Yuldoshov, *Aquaculture*, 2025, **595**, 741661.
162 Z. Hu, M. Chen, C. Zhang, Z. Li, M. Feng, L. Wu, M. Zhou and D. Liang, *Biosensors*, 2022, **12**, 268.
163 Y. Wei, Z. Yang, C. Zong, B. Wang, X. Ge, X. Tan, X. Liu, Z. Tao, P. Wang and C. Ma, *Angew. Chem.*, 2021, **133**, 24443–24449.
164 Z. Chi, Y. Wu, L. Chen, H. Yang, M. R. Khan, R. Busquets, N. Huang, X. Lin, R. Deng and W. Yang, *Anal. Chim. Acta*, 2022, **1205**, 339763.
165 A. Santiago-Frangos, L. N. Hall, A. Nemudraia, A. Nemudryi, P. Krishna, T. Wiegand, R. A. Wilkinson, D. T. Snyder, J. F. Hedges and C. Cicha, *Cell Rep. Med.*, 2021, **2**(6), 100319.
166 J. A. Steens, Y. Zhu, D. W. Taylor, J. P. Bravo, S. H. Prinsen, C. D. Schoen, B. J. Keijser, M. Ossendrijver, L. M. Hofstra and S. J. Brouns, *Nat. Commun.*, 2021, **12**, 5033.
167 S. Grüschow, C. S. Adamson and M. F. White, *Nucleic Acids Res.*, 2021, **49**, 13122–13134.
168 S. Grüschow, P. C. Steketee, E. Paxton, K. R. Matthews, L. J. Morrison, M. F. White and F. Grey, *PLoS Neglected Trop. Dis.*, 2025, **19**, e0012937.
169 Z. Yu, J. Xu and Q. She, *Int. J. Mol. Sci.*, 2023, **24**, 2857.
170 C. Rouillon, J. S. Athukoralage, S. Graham, S. Grüschow and M. F. White, *eLife*, 2018, **7**, e36734.
171 Q. He, X. Lei, Y. Liu, X. Wang, N. Ji, H. Yin, H. Wang, H. Zhang and G. Yu, *ChemBioChem*, 2023, **24**, e202300401.
172 M. Zhang, X. Zhang, Y. Xu, Y. Xiang, B. Zhang, Z. Xie, Q. Wu and C. Lou, *Nat. Commun.*, 2024, **15**, 8768.
173 K. Asano, K. Yoshimi, K. Takeshita, S. Mitsuhashi, Y. Kochi, R. Hirano, Z. Tingyu, S. Ishida and T. Mashimo, *ACS Synth. Biol.*, 2024, **13**(12), 3926–3935.
174 T. Hu, Q. Ji, X. Ke, H. Zhou, S. Zhang, S. Ma, C. Yu, W. Ju, M. Lu and Y. Lin, *Commun. Biol.*, 2024, **7**, 858.
175 A. Nemudraia, A. Nemudryi, M. Buyukyoruk, A. M. Scherffius, T. Zahl, T. Wiegand, S. Pandey, J. E. Nichols, L. N. Hall and A. McVey, *Nat. Commun.*, 2022, **13**, 7762.
176 M. Paraan, M. Nasef, L. Chou-Zheng, S. A. Khweis, A. J. Schoeffler, A. Hatoum-Aslan, S. M. Stagg and J. A. Dunkle, *PLoS One*, 2023, **18**, e0287461.
177 P. Samai, N. Pyenson, W. Jiang, G. W. Goldberg, A. Hatoum-Aslan and L. A. Marraffini, *Cell*, 2015, **161**, 1164–1174.
178 P. Lin, G. Shen, K. Guo, S. Qin, Q. Pu, Z. Wang, P. Gao, Z. Xia, N. Khan and J. Jiang, *Nucleic Acids Res.*, 2022, **50**, e47.
179 M. Chen, X. Jiang, Q. Hu, J. Long, J. He, Y. Wu, Z. Wu, Y. Niu, C. Jing and X. Yang, *ACS Sens.*, 2023, **9**, 62–72.
180 C. Hu, D. Ni, K. H. Nam, S. Majumdar, J. McLean, H. Stahlberg, M. P. Terns and A. Ke, *Mol. Cell*, 2022, **82**, 2754–2768.
181 B. Spanjaard, B. Hu, N. Mitic, P. Olivares-Chauvet, S. Janjuha, N. Ninov and J. P. Junker, *Nat. Biotechnol.*, 2018, **36**, 469–473.
182 K. Pardee, A. A. Green, M. K. Takahashi, D. Braff, G. Lambert, J. W. Lee, T. Ferrante, D. Ma, N. Donghia and M. Fan, *Cell*, 2016, **165**, 1255–1266.
183 J. Chen, Y. Chen, L. Huang, X. Lin, H. Chen, W. Xiang and L. Liu, *Nat. Biotechnol.*, 2024, 1–11.
184 D. Huang, Z. Shi, J. Qian, K. Bi, M. Fang and Z. Xu, *Biotechnol. Bioeng.*, 2021, **118**, 1568–1577.
185 A. Kumaran, N. J. Serpes, T. Gupta, A. James, A. Sharma, D. Kumar, R. Nagraik, V. Kumar and S. Pandey, *Biosensors*, 2023, **13**(2), 202.
186 N. Mohammad, A. Steksova, Y. Tang, L. Huang, A. Velayati, S. Zhang, A. Dey Poonam, S. Jamalzadegan, M. Breen and G. Jiang, *bioRxiv*, 2025, preprint, DOI: **10.1101/2025.06.15.659809**.
187 X. Li, B. Su, L. Yang, Z. Kou, H. Wu, T. Zhang, L. Liu, Y. Han, M. Niu and Y. Sun, *BMC Infect. Dis.*, 2023, **23**, 627.
188 P. Chen, M. Chen, Y. Chen, X. Jing, N. Zhang, X. Zhou, X. Li, G. Long and P. Hao, *Virus Res.*, 2022, **312**, 198707.
189 M. Bagi, F. Amjad, S. M. Ghoreishian, S. Sohrabi Shahsavari, Y. S. Huh, M. K. Moraveji and S. Shimpalee, *BioChip J.*, 2024, 1–23.
190 X. Xu, Y. Zhang, J. Liu, S. Wei, N. Li, X. Yao, M. Wang, X. Su, G. Jing and J. Xu, *ACS Nano*, 2024, **19**, 1271–1285.
191 X. Ma, F. Zhou, D. Yang, Y. Chen, M. Li and P. Wang, *Anal. Chem.*, 2023, **95**, 13220–13226.
192 G. Lee, O. Hossain, S. Jamalzadegan, Y. Liu, H. Wang, A. C. Saville, T. Shymanovich, R. Paul, D. Rotenberg and A. E. Whitfield, *Sci. Adv.*, 2023, **9**, eade2232.
193 O. Hossain, Y. Wang, M. Li, B. Mativenga, S. Jamalzadegan, N. Mohammad, A. Velayati, A. D. Poonam and Q. Wei, *Biosens. Bioelectron.*, 2025, **278**, 117341.
194 S. Jamalzadegan, J. Xu, Y. Shen, B. Mativenga, M. Li, M. Zare, A. Penumudy, Z. Hetzler, Y. Zhu and Q. Wei, *Chem Bio Eng.*, 2025, **5**(3), e00027.
195 Z. Hetzler, Y. Wang, D. Krafft, S. Jamalzadegan, L. Overton, M. W. Kudenov, F. S. Ligler and Q. Wei, *Front. Chem.*, 2022, **10**, 983523.
196 T. Tanny, M. Sallam, N. Soda, N.-T. Nguyen, M. Alam and M. J. Shiddiky, *J. Agric. Food Chem.*, 2023, **71**, 11765–11788.
197 S. G. Jaybhaye, R. L. Chavhan, V. R. Hinge, A. S. Deshmukh and U. S. Kadam, *Virology*, 2024, 110160.
198 W. Zhang, Y. Jiao, C. Ding, L. Shen, Y. Li, Y. Yu, K. Huang, B. Li, F. Wang and J. Yang, *Front. Microbiol.*, 2021, **12**, 745173.
199 O. O. Abudayyeh, J. S. Gootenberg, M. J. Kellner and F. Zhang, *CRISPR J.*, 2019, **2**, 165–171.
200 J. M. Bernabé-Orts, Y. Hernando and M. A. Aranda, *PhytoFrontiers™*, 2022, **2**, 92–100.
201 M.-C. Marqués, J. Sánchez-Vicente, R. Ruiz, R. Montagud-Martínez, R. Márquez-Costa, G. Gómez, A. Carbonell, J.-A. Daròs and G. Rodrigo, *ACS Synth. Biol.*, 2022, **11**, 2384–2393.
202 X. Duan, W. Ma, Z. Jiao, Y. Tian, R. G. Ismail, T. Zhou and Z. Fan, *Phytopathol. Res.*, 2022, **4**, 23.
203 A. K. Wani, N. Akhtar, C. Chopra, R. Singh, J. C. Hong and U. S. Kadam, *Environ. Technol. Innovation*, 2024, **34**, 103625.
204 B. Durán-Vinet, K. Araya-Castro, A. Zaiko, X. Pochon, S. A. Wood, J.-A. L. Stanton, G.-J. Jeunen, M. Scriver, A. Kardailsky and T.-C. Chao, *CRISPR J.*, 2023, **6**, 316–324.
205 Targeting miRNA by CRISPR/Cas in cancer: advantages and challenges|Military Medical Research, **https://link.springer.com/article/10.1186/s40779-023-00468-6**, (accessed April 30, 2025).
206 Y. Zhou and S.-J. Chen, *Artif. Intell. Chem.*, 2024, **2**, 100053.
207 H. Xiao, X. Yang, Y. Zhang, Z. Zhang, G. Zhang and B.-T. Zhang, *RNA Biol.*, 2023, **20**, 384–397.
208 M. Hu, R. Liu, Z. Qiu, F. Cao, T. Tian, Y. Lu, Y. Jiang and X. Zhou, *Angew. Chem.*, 2023, **135**, e202300663.
209 X. Zhang, F. Li, X. Li, G. Tian and Q. Xia, *Sens. Actuators, B*, 2025, 138074.
210 Y. Wan, S. Li, W. Xu, K. Wang, W. Guo, C. Yang, X. Li, J. Zhou and J. Wang, *Anal. Chem.*, 2024, **96**, 16346–16354.
211 A. M. Ekdahl, A. M. Rojano-Nisimura and L. M. Contreras, *J. Mol. Biol.*, 2022, **434**, 167689.
212 Y. Wu, W. Luo, Z. Weng, Y. Guo, H. Yu, R. Zhao, L. Zhang, J. Zhao, D. Bai and X. Zhou, *Nucleic Acids Res.*, 2022, **50**, 11727–11737.
213 U. S. Kadam, Y. Cho, T. Y. Park and J. C. Hong, *Appl. Biol. Chem.*, 2023, **66**, 13.
214 S. Gong, X. Wang, P. Zhou, W. Pan, N. Li and B. Tang, *Anal. Chem.*, 2022, **94**, 15839–15846.
215 S. Del Giovane, N. Bagheri, A. C. Di Pede, A. Chamorro, S. Ranallo, D. Migliorelli, L. Burr, S. Paoletti, H. Altug and A. Porchetta, *TrAC, Trends Anal. Chem.*, 2024, **172**, 117594.
216 Portable CRISPR-based diagnostics|Nature Biotechnology, **https://www.nature.com/articles/s41587-019-0220-1**, (accessed April 30, 2025).

217 I. Hernández-Neuta, F. Neumann, J. Brightmeyer, T. Ba Tis, N. Madaboosi, Q. Wei, A. Ozcan and M. Nilsson, *J. Intern. Med.*, 2019, **285**, 19–39.
218 J. C. Contreras-Naranjo, Q. Wei and A. Ozcan, *IEEE J. Sel. Top. Quantum Electron.*, 2015, **22**, 1–14.
219 R. Paul, E. Ostermann and Q. Wei, *Biosens. Bioelectron.*, 2020, **169**, 112592.
220 Scalable and automated CRISPR-based strain engineering using droplet microfluidics|Microsystems & Nanoengineering, **https://www.nature.com/articles/s41378-022-00357-3**, (accessed April 30, 2025).
221 M. A. Ahamed, A. J. Politza, T. Liu, M. A. U. Khalid, H. Zhang and W. Guan, *Nanotechnology*, 2025, **36**, 042001.
222 A thermostable type I-B CRISPR–Cas system for orthogonal and multiplexed genetic engineering|Nature Communications, **https://www.nature.com/articles/s41467-023-41973-5**, (accessed April 30, 2025).
223 K. H. Morelli, Q. Wu, M. L. Gosztyla, H. Liu, M. Yao, C. Zhang, J. Chen, R. J. Marina, K. Lee, K. L. Jones, M. Y. Huang, A. Li, C. Smith-Geater, L. M. Thompson, W. Duan and G. W. Yeo, *Nat. Neurosci.*, 2023, **26**, 27–38.
224 Y. Li, L. Zhao, W. Kang, L. Ma, Y. Bai and F. Feng, *TrAC, Trends Anal. Chem.*, 2025, **191**, 118329.
225 H.-C. Kuo, J. Prupes, C.-W. Chou and I. J. Finkelstein, *Nat. Commun.*, 2024, **15**, 498.

